

## Cyclopentadienyl Ruthenium(II) Complexes with Bridging Alkynylphosphine Ligands: Synthesis and Electrochemical Studies

Barbara Di Credico,<sup>[a]</sup> Fabrizia Fabrizi de Biani,<sup>[b]</sup> Luca Gonsalvi,<sup>[a]</sup> Annalisa Guerri,<sup>[c]</sup> Andrea Ienco,<sup>[a]</sup> Franco Laschi,<sup>[b]</sup> Maurizio Peruzzini,<sup>\*,[a]</sup> Gianna Reginato,<sup>[a]</sup> Andrea Rossin,<sup>[a]</sup> and Piero Zanello<sup>[b]</sup>

*Dedicated to the Centenary of the Italian Chemical Society*

**Abstract:** The reaction of  $[\text{CpRuCl}(\text{PPh}_3)_2]$  (Cp = cyclopentadienyl) and  $[\text{CpRuCl}(\text{dppe})]$  (dppe =  $\text{Ph}_2\text{PCH}_2\text{CH}_2\text{PPh}_2$ ) with bis- and triphosphine ligands 1,4-( $\text{Ph}_2\text{PC}\equiv\text{C}$ ) $_2\text{C}_6\text{H}_4$  (**1**) and 1,3,5-( $\text{Ph}_2\text{PC}\equiv\text{C}$ ) $_3\text{C}_6\text{H}_3$  (**2**), prepared by Ni-catalysed cross-coupling reactions between terminal alkynes and diphenylchlorophosphine, has been investigated. Using metal-directed self-assembly methodologies, two linear bimetallic complexes,  $[\{\text{CpRuCl}(\text{PPh}_3)_2(\mu\text{-dppab})\}]$  (**3**) and  $[\{\text{CpRu}(\text{dppe})_2(\mu\text{-dppab})\}(\text{PF}_6)_2]$  (**4**), and the mononuclear complex  $[\text{CpRuCl}(\text{PPh}_3)(\eta^1\text{-dppab})]$  (**6**), which contains a “dangling arm” ligand, were prepared (dppab = 1,4-bis[(diphenylphosphino)ethynyl]benzene). More-

over, by using the triphosphine 1,3,5-tris[(diphenylphosphino)ethynyl]benzene (tppab), the trimetallic  $[\{\text{CpRuCl}(\text{PPh}_3)_3(\mu_3\text{-tppab})\}]$  (**5**) species was synthesised, which is the first example of a chiral-at-ruthenium complex containing three different stereogenic centres. Besides these open-chain complexes, the neutral cyclic species  $[\{\text{CpRuCl}(\mu\text{-dppab})_2\}]$  (**7**) was also obtained under different experimental conditions. The coordination chemistry of such systems towards supramolecular assemblies was

tested by reaction of the bimetallic precursor **3** with additional equivalents of ligand **2**. Two rigid macrocycles based on *cis* coordination of dppab to  $[\text{CpRu}(\text{PPh}_3)]$  were obtained, that is, the dinuclear complex  $[\{\text{CpRu}(\text{PPh}_3)(\mu\text{-dppab})_2\}(\text{PF}_6)_2]$  (**8**) and the tetranuclear square  $[\{\text{CpRu}(\text{PPh}_3)(\mu\text{-dppab})_4\}(\text{PF}_6)_4]$  (**9**). The solid-state structures of **7** and **8** have been determined by X-ray diffraction analysis and show a different arrangement of the two parallel dppab ligands. All compounds were characterised by various methods including ESIMS, electrochemistry and by X-band ESR spectroscopy in the case of the electrogenerated paramagnetic species.

**Keywords:** electrochemistry • phosphane ligands • polynuclear complexes • ruthenium • X-ray diffraction

### Introduction

The incorporation of metal atoms into supramolecular assemblies is considered to be an efficient pathway for the development of new functional materials with novel physical and chemical properties.

In particular, transition-metal centres may introduce Lewis acidity,<sup>[1]</sup> magnetism,<sup>[2]</sup> redox activity<sup>[3]</sup> or luminescence<sup>[4]</sup> properties into metallopolymers and macrocyclic structures. The synthesis of metallomacrocycles represents an interesting area to explore the development of “host-guest” chemistry. These species contain large cavities that can be occupied by small guest molecules that can in turn modify the chemical properties and reactivity of the host molecule. Furthermore, macrocyclic molecular squares, rectangles or boxes have been prepared for applications in

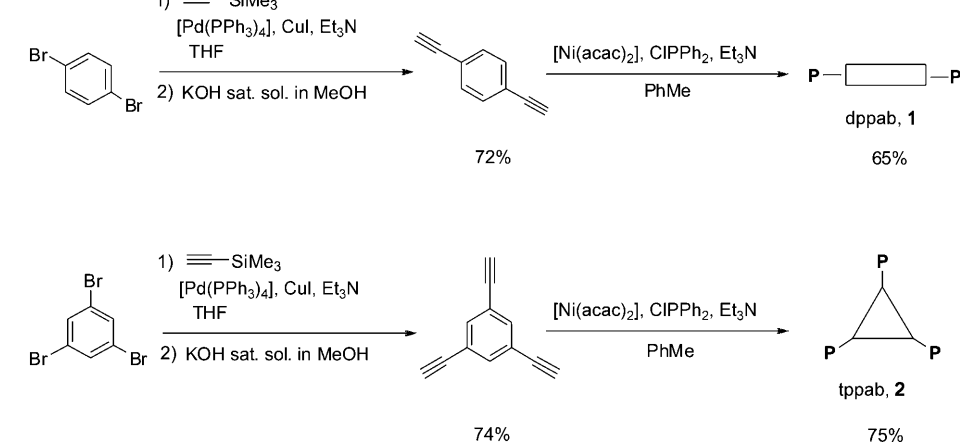
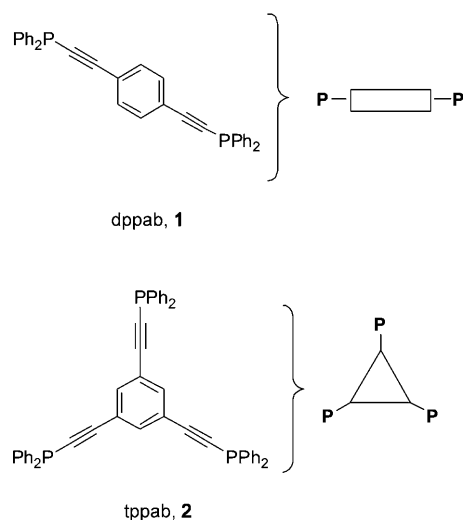
[a] Dipl.-Chem. B. Di Credico, Dr. L. Gonsalvi, Dr. A. Ienco, Dr. M. Peruzzini, Dr. G. Reginato, Dr. A. Rossin  
Istituto di Chimica dei Composti OrganoMetallici ICCOM  
Consiglio Nazionale delle ricerche CNR  
via Madonna del Piano 10, 50019 Sesto Fiorentino, Florence (Italy)  
Fax: (+39)055-5225203  
E-mail: m.peruzzini@iccom.cnr.it

[b] Dr. F. Fabrizi de Biani, Prof. Dr. F. Laschi, Prof. Dr. P. Zanello  
Dipartimento di Chimica, Università degli Studi di Siena  
via A. De Gasperi 2, 53100, Siena (Italy)

[c] Dr. A. Guerri  
Dipartimento di Chimica, Università degli Studi di Firenze  
via della Lastruccia 3, 50019, Sesto Fiorentino, Florence (Italy)

areas such as molecular recognition, sensing and modelling for biological systems.<sup>[5]</sup>

Ligands containing two or more metal-binding phosphorus donor atoms are versatile building blocks for the construction of linear or cross-linked complexes by self-assembly of ditopic or multitopic units with metal ions.<sup>[6]</sup> Although the use of alkenyl and alkynylphosphines has precedents in the coordination chemistry of a wide range of transition metals,<sup>[7,8]</sup> ruthenium(II) complexes bearing these ligands are rare.<sup>[9]</sup> Remarkably, the only complex containing a di-phosphinoalkyne ligand is Dyson's compound  $[(p\text{-cymene})\text{RuCl}_2]_x(\text{dppa})$  ( $x=1,2$ ; dppa = diphenylphosphinoacetylene).<sup>[10]</sup> With the aim of expanding on this theme and these architectures, we report here results on the synthesis and structural characterisation of a family of cyclopentadienyl ruthenium(II) (CpRu) complexes with the bi- and tridentate phosphines 1,4-bis[(diphenylphosphino)ethynyl]benzene (dppab, **1**) and 1,3,5-tris[(diphenylphosphino)ethynyl]benzene (tppab, **2**, and Scheme 1).



Scheme 1. Synthesis of the bidentate and tridentate ligands dppab **1** and tppab **2**.

The dppab and tppab rigid ligands are significantly more functionalised than those that contain merely acetylene as a spacer (like dppa, diphenylphosphinoacetylene),<sup>[11]</sup> which could help to spontaneously assemble large macrocyclic systems instead of discrete complexes. In addition, the presence of C≡C triple bonds conjugated with an aromatic ring could favour an effective electronic communication between the different metal centres held together by the alkynylphosphino bridge. Using metal-directed self-assembly methodologies, two linear bimetallic complexes,  $[\{\text{CpRuCl}(\text{PPh}_3)_2(\mu\text{-dppab})\}]$  (**3**) and  $[\{\text{CpRu}(\text{dppe})_2(\mu\text{-dppab})\}](\text{PF}_6)_2$  (**4**), and the trimetallic  $[\{\text{CpRuCl}(\text{PPh}_3)_3(\mu_3\text{-tppab})\}]$  (**5**) species (dppe = 1,2-bis(diphenylphosphino)ethane) were prepared and fully characterised. Moreover, the mononuclear complex  $[\text{CpRuCl}(\text{PPh}_3)(\eta^1\text{-dppab})]$  (**6**) that contains a “dangling” diphosphine arm was synthesised, thereby showing that ligand **1** may exhibit either  $\mu\text{-}\eta^2$ - (end-on) or  $\eta^1$ -coordination modes. Besides these open-chain complexes, the neutral cyclic species  $[\{\text{CpRuCl}(\mu\text{-dppab})\}_2]$  (**7**) was also obtained under different experimental conditions. Finally, the pre-assembled metal-based mono- and dinuclear moieties mentioned above were used as starting materials to prepare metallomacrocycles of diverse shapes and sizes. Thus, self-assembly of the dimetal precursor **3** with additional equivalents of dppab led to an approximately 1:1 mixture of the cyclic dimer  $[\{\text{CpRu}(\text{PPh}_3)(\mu\text{-dppab})\}_2](\text{PF}_6)_2$  (**8**) and the tetramer  $[\{\text{CpRu}(\text{PPh}_3)(\mu\text{-dppab})\}_4](\text{PF}_6)_4$  (**9**). These rigid macrocycles based on *cis* ligation of the  $\{\text{CpRu}(\text{PPh}_3)\}$  moiety belong to the growing family of polynuclear compounds with potential applications in host-guest, inclusion, and molecular recognition chemistry.<sup>[12]</sup> Apart from elemental analysis, routine chemico-physical characterisation (multinuclear NMR and FTIR spectroscopy) and single-crystal X-ray diffraction data collection on selected complexes, all of the compounds were analysed through ESIMS, electrochemical methods and, for the electrogenerated paramagnetic species, by X-band ESR spectroscopy.

## Results and Discussion

**Synthesis and characterisation of the alkynylphosphine ligands:** Although ligands **1**<sup>[13]</sup> and **2**<sup>[8]</sup> have been already described, we report here on a new synthetic pathway that does not request the use of highly reactive sodium, lithium or magnesium ethynyl reagents and also provides better yields of both alkynylphosphines. Thus, dppab (**1**) and tppab (**2**) were prepared from the corresponding terminal alkynes by a Ni-catalyzed cross-coupling reaction with chlorodiphenyl-

phosphine in the presence of  $\text{NEt}_3$  (Scheme 1). The Sonogashira reaction of aryl bromides with trimethylsilyl acetylene is used to prepare the terminal alkyne, after hydrolysis of the  $\text{SiMe}_3$  protecting groups. The use of halophosphines  $\text{R}_2\text{PX}^{[14]}$  represents a synthetic approach, based on an umpolung process alternative to the literature methods, for example, the reaction of secondary phosphine  $\text{R}_2\text{PH}$  with  $\text{R-X}$  substrates including halogenated alkynes.<sup>[15]</sup>

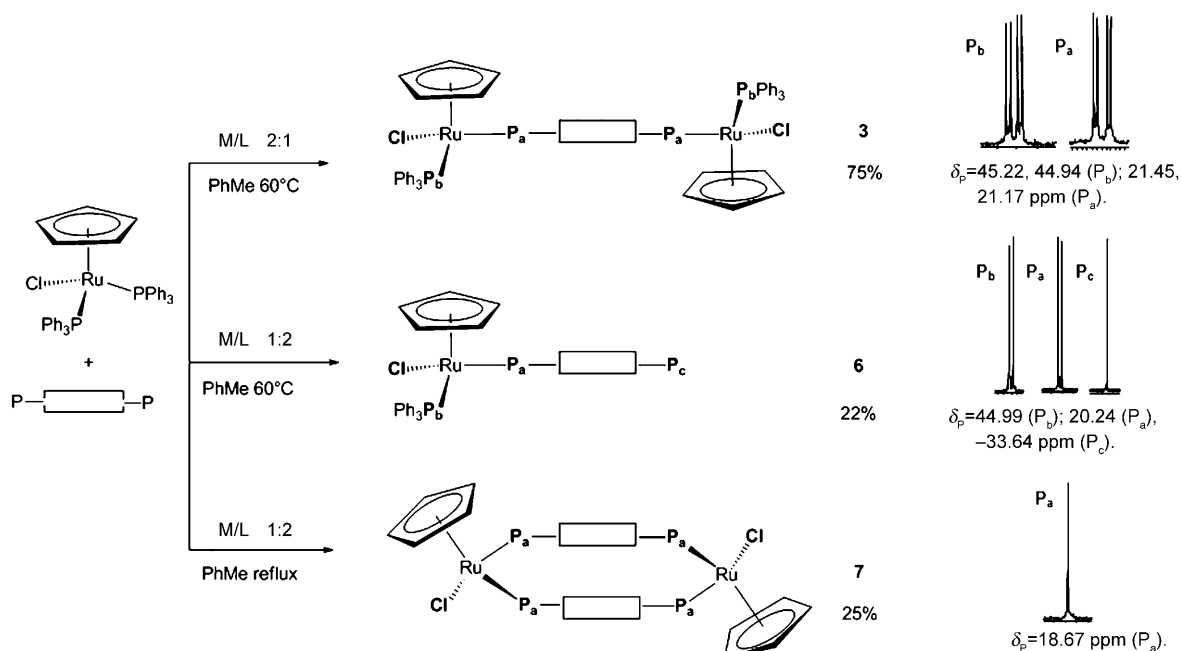
The classical synthesis of alkynylphosphines often involves direct lithiation of the terminal  $\text{C}\equiv\text{C-H}$  bond, followed by reaction of the in situ generated acetylide carbanion with  $\text{R}_2\text{PX}$ .<sup>[8,16]</sup> Although the latter preparative methodology was also used in this work, the yields of the alkynylphosphines were always significantly lower, so our alternative method was preferred.

**Synthesis and characterisation of neutral ruthenium complexes with dppab:** To explore the coordination properties of these alkynylphosphines towards transition metals, we investigated the reactivity of both **1** and **2** with a variety of  $\text{Ru}^{\text{II}}$  precursors. The easy-to-make, readily available and stable  $\text{Ru}^{\text{II}}$  complex  $[\text{CpRuCl}(\text{PPh}_3)_2]$  (**10**)<sup>[17]</sup> gave the best results. Several attempts were made also using other  $\text{Ru}^{\text{II}}$  precursors such as  $[\text{CpRu}(\eta^6\text{-C}_{10}\text{H}_8)(\text{PF}_6)]$ ,  $[\{(\eta^6\text{-}p\text{-cymene})\text{RuCl}_2\}_2]$  and  $[\text{Ru}(\text{PPh}_3)_3\text{Cl}_2]$ . Irrespective of the precursor used, mixtures of several products were formed, and neither simple  $^{31}\text{P}$  NMR identification nor isolation of pure products after workup was possible. Thus, the reactivity of both **1** and **2** with these  $\text{Ru}^{\text{II}}$  precursors was not investigated further.

As a general consideration, the ruthenium complexes of the polyphosphines here described are moderately air-

stable, and can be handled in air without special precautions, although they are better stored under nitrogen. The observed stability towards air oxidation made column chromatographic techniques suitable for the final purification of the neutral  $\text{CpRu}$  derivatives, which could therefore be obtained as analytically pure microcrystalline materials (see the Experimental Section). Phosphine exchange at the metal centre in precursor **10** or halide abstraction using  $\text{TIPF}_6$  in the presence of an additional ligand were the methodologies used to prepare the  $\text{Ru}^{\text{II}}$  complexes. The reaction temperature and the metal-to-ligand molar ratio were the most important factors to influence the reaction outcome, hence the nature of the obtained products.

In a first experiment aimed at preparing coordination complexes that exploited both donor ends of the biphosphine **1**, a 2:1 M/L ratio was employed and the reaction was carried out at  $60^\circ\text{C}$  in toluene. The reaction resulted in the immediate formation ( $^{31}\text{P}\{^1\text{H}\}$  NMR spectroscopic monitoring) of the bimetallic complex **3**, which could be isolated and purified in excellent yield as an orange microcrystalline powder after chromatographic workup (Scheme 2). Remarkably, both  $\text{Ru}$  centres in **3** are stereogenic due to the presence of four different substituents on a distorted piano-stool-coordinated polyhedron. In keeping with such stereochemical arrangement, the  $^{31}\text{P}\{^1\text{H}\}$  NMR spectrum of **3** shows two pairs of 1:1 doublets.<sup>[18]</sup> Correspondingly, two distinct and partially overlapped peaks can be observed in the  $\text{Cp}$  region of the  $^1\text{H}$  NMR spectrum, thus confirming the formation of a pair of enantiomers ( $R_{\text{Ru}}, R_{\text{Ru}}$  and  $S_{\text{Ru}}, S_{\text{Ru}}$ ) together with the *meso* form ( $R_{\text{Ru}}, S_{\text{Ru}}$  and  $S_{\text{Ru}}, R_{\text{Ru}}$ ). When a solution of **3** in  $[\text{D}_3]$ acetonitrile was warmed to  $80^\circ\text{C}$  (NMR spectroscopy tube test), no significant change in the intensi-



Scheme 2. Synthesis of dppab complexes **3**, **6** and **7**. The related  $^{31}\text{P}\{^1\text{H}\}$  NMR spectroscopic signals are shown on the right side of the scheme.

ty ratio of the two pairs of doublets was observed, thereby proving the absence of any dynamic process that could have been expected from a pair of equilibrating rotamers. The simultaneous presence of two stereogenic metal atoms in a bimetallic complex is quite rare;<sup>[19,20]</sup> chiral (carbon) centres are normally located on the ligands. Resolution of the diastereomeric mixture by means of the chromatographic techniques was impossible, due to the almost identical  $R_f$  values of the diastereoisomers (dichloromethane/acetone 20:1).

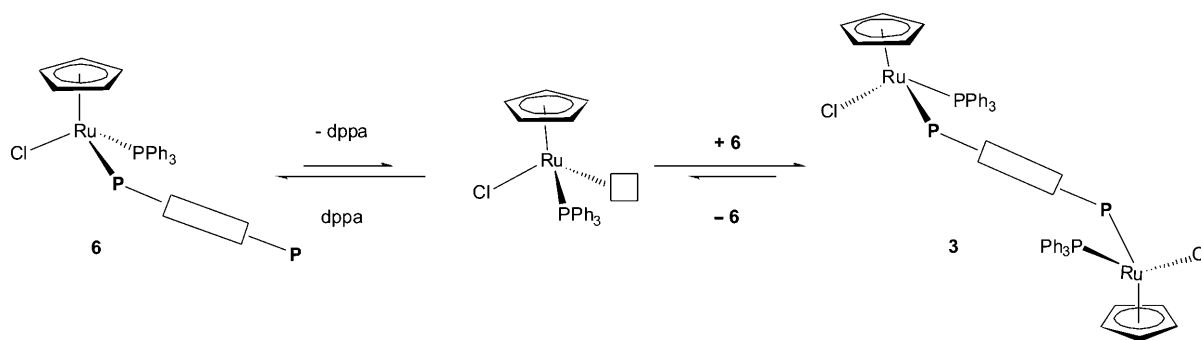
The reaction was repeated using an M/L ratio of 1:2. In this case, an equilibrium mixture between the species **6**, **3** and **1** was observed. Among these products, complex **6**, which contained a dangling, uncoordinated diphosphine arm, was the main product in the reaction crude. The overall low yield of isolated **6** after workup (22%) likely reflects its participation in a room temperature equilibrium, thereby giving the bridged species **3** through dppab dissociation followed by reaction of the coordinatively unsaturated {CpRuCl(PPh<sub>3</sub>)} unit with a second equivalent of **6** (Scheme 3). Notably, the ligand redistribution (**6**)+(6) $\rightleftharpoons$ (**1**)+(3) in solution did not permit the collection of exhaustive ESIMS data for **6**. The process can be followed by <sup>31</sup>P{<sup>1</sup>H} NMR spectroscopy, which shows that as the signals belonging to **6** decrease, those ascribable to free **1** and complex **3** grow in parallel. A similar behaviour was also recently observed by Dyson et al. for the Ru<sup>II</sup> complex [( $\eta^6$ -p-cymene)RuCl<sub>2</sub>( $\eta^1$ -dppa)], which also contains a bridging bidentate phosphine.<sup>[10]</sup>

A solution of a 1:2 ratio between [CpRu(PPh<sub>3</sub>)<sub>2</sub>Cl] and **1** in toluene heated at reflux did not yield **6**, but rather gave the diruthenamacrocycle **7** as a single stable thermodynamic

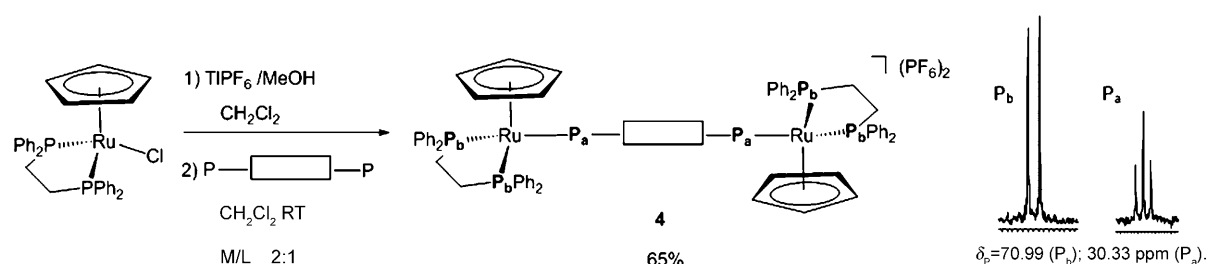
product. Complex **7** is likely to form through intermolecular thermal replacement of the triphenylphosphine ligand in **6** by the pending P donor atom of a second equivalent of the same ruthenium complex. Due to the presence of identical phosphine ligands, no chirality at Ru was observed, which is in line with the presence of a singlet resonance in the <sup>31</sup>P{<sup>1</sup>H} NMR spectrum ( $\delta$ =18.67 ppm). Complex **7** belongs to the known family of diruthenium complexes in which two {CpRuL} moieties (L= $\sigma$ -donor ligand) are held together by a pair of bidentate ligands.<sup>[20,21]</sup>

### Synthesis and characterisation of cationic ruthenium complexes of dppab:

Removal of the chloride ligand in {CpRuCl} species during the reaction with dppab could easily favour the formation of either dinuclear cationic complexes or macrocyclic species depending on the nature of the ruthenium precursor and the stoichiometric ratio. This possibility was firstly explored by using the precursor [CpRuCl(dppe)] (**11**), which contains the chelating ancillary diphosphine 1,2-diphenylphosphinoethane (dppe) instead of two monodentate phosphines such as PPh<sub>3</sub>. Using TlPF<sub>6</sub> in CH<sub>2</sub>Cl<sub>2</sub>/MeOH at ambient temperature as effective halide scavenger on a 2:1 M/L solution afforded as expected the bridged product **4** in quantitative NMR spectroscopic yield (Scheme 4). Complex **4** shares with **3** the main structural motif in which two {CpRu(dppe)} cations are held together by a bridging dppab ligand. The most intriguing difference between the two complexes is, apart from the cationic versus neutral nature, the lack of stereogenicity at the metal centres due to the presence of dppe chelating ligands.



Scheme 3. Proposed mechanism for the (**6**)+(6) $\rightleftharpoons$ (**1**)+(3) reaction.



Scheme 4. Synthesis of the dinuclear complex **4**. The related <sup>31</sup>P{<sup>1</sup>H} NMR spectroscopic signals are shown on the right side of the scheme.

As **3** does not contain the sterically forcing dppe chelate, addition of  $\text{TIPF}_6$  to a solution of **3** in the presence of an additional equivalent of dppab is an efficient way to grow polynuclear macrocyclic complexes featuring a 1:1 M/L ratio. Thus, removal of the chloride ligand from a solution of **3** in dichloromethane with  $\text{TIPF}_6$  did not provide any defined product unless the reaction was carried out in the presence of dppab. Workup of the solution after filtering out  $\text{TiCl}_4$  gave a dark orange powder consisting of an approximate 1:1 mixture of complexes **8** and **9**, which were assigned as dinuclear  $[\text{M}^2\text{L}_2]^{2+}$  and tetranuclear  $[\text{M}^4\text{L}_4]^{4+}$  species (Scheme 5).

The formation of discrete macrocycles of formula  $[\text{cyclo}\{-\text{CpRu}(\text{PPh}_3)(\mu,\eta^{1-1}\text{-dppab})\}_n]$  ( $n=2, 4$ ) which was favoured with respect to open-chain metallorganic polymers  $\{\text{CpRu}(\text{PPh}_3)(\mu,\eta^{1-1}\text{-dppab})\}_\infty$  may be due to enthalpic effects.<sup>[22,23]</sup> In turn, entropic factors would favour the formation of small cycles over larger ones.<sup>[23]</sup> However, in the case at hand, the observed 1:1 ratio between **8** and **9** may find its explanation in the rigidity of dppab and the nearly  $90^\circ$  L-Ru-L bond angle ( $95.53^\circ$  for **8**, see below), which would lead to the thermodynamically most stable square arrangement featured by **9**. A similar behaviour has been documented by Rheingold and co-workers for a family of Re-Pd polymetal-lamacrocycles.<sup>[12]</sup> Complexes **8** and **9** were separated by fractional crystallisation from a diluted dichloromethane/*n*-hexane solution from which analytically pure samples of **8** and **9** were obtained as dark orange and yellow microcrystals, respectively. The proposed

formulas were unambiguously confirmed by a combination of chemico-physical data including elemental analysis, molar conductivity in solution, mass spectral and multinuclear NMR spectroscopy. Particularly significant was the  $^{31}\text{P}\{^1\text{H}\}$  NMR spectrum showing two practically superimposed  $\text{AM}_2$  spin systems, which provide confirmatory evidence for the coordination of two different dppab ligands to each  $\{\text{CpRu}(\text{PPh}_3)\}$  moiety (top trace in Figure 1). Thus, while **8** showed a high-frequency triplet ( $\delta_{\text{P}}=38.95$  ppm) and a lower frequency doublet ( $\delta_{\text{P}}=20.26$  ppm) with  $^2J(\text{P,P})=37.5$  Hz), the tetramer **9** exhibited a doublet at  $\delta=223.88$  ppm and a slightly highfield-shifted triplet ( $\delta_{\text{P}}=39.23$  ppm;  $^2J(\text{P,P})=38.5$  Hz), in accordance with the proposed structures (Scheme 5).

To assess the dimeric versus tetrameric nature of **8** and **9**, respectively, the high-resolution ESIMS spectra of the two complexes were of importance. In particular, **9** exhibits an  $[\text{M}-2\text{PF}_6]^{2+}$  signal at  $m/z$  1991.3; its experimental isotopic

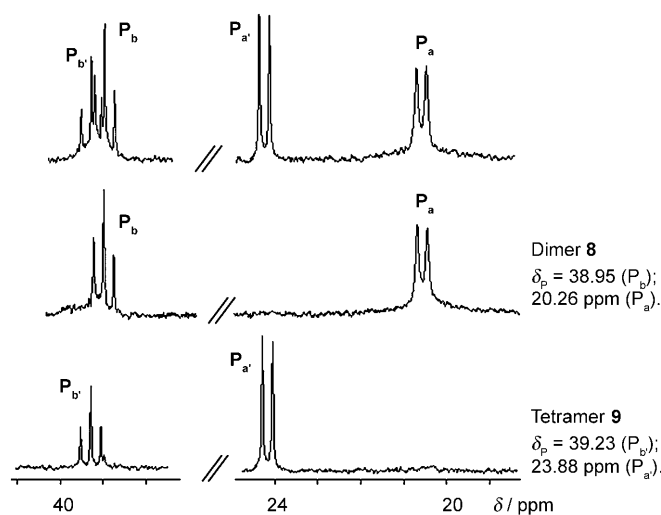
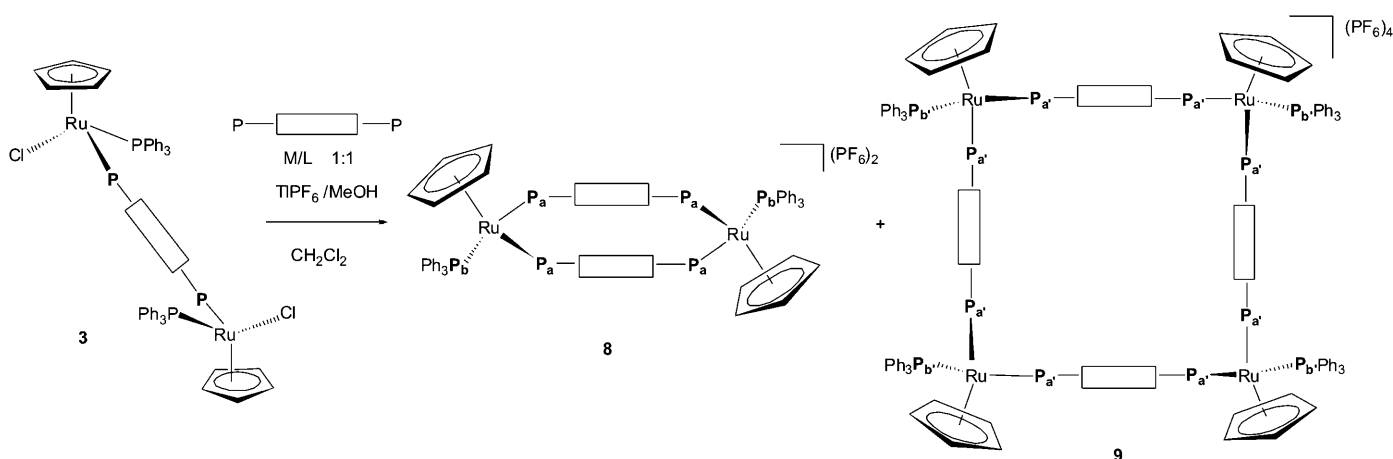


Figure 1.  $^{31}\text{P}\{^1\text{H}\}$  NMR ( $\text{CD}_2\text{Cl}_2$ ) spectrum of the crude reaction mixture **6**/ $\text{TIPF}_6$ /dppab consisting of **8** and **9** (top) and the  $\text{AM}_2$  patterns due to the isolated complexes (**8**, middle; **9**, bottom).



Scheme 5. Synthesis of complexes **8** and **9**.

pattern matches the calculated values well (Figure 2), thus validating the tetranuclear nature of this interesting ruthena-macrocycle.

To explore the stability of the polymetallic species **8** and **9** and, most importantly, to verify whether any equilibration could account for the interconversion of **9** into **8**,  $^{31}\text{P}\{^1\text{H}\}$  NMR spectra in  $\text{CD}_3\text{CN}$  were recorded at different temperatures. Thus, warming a solution of **8** in  $[\text{D}_3]\text{acetonitrile}$  to  $80^\circ\text{C}$  did not show any transformation suggesting that **9** does not originate from the intermolecular aggregation of two dinuclear dications **8**. Similarly, the  $^{31}\text{P}\{^1\text{H}\}$  NMR spectrum of a solution of tetramer **9** in  $\text{CD}_3\text{CN}$  does not change on increasing the temperature from  $20$  to  $80^\circ\text{C}$ . These results are mechanistically relevant because they suggest that the two compounds do not take part in equilibria, hence they should be generated through different reaction pathways. Remarkably, this behaviour contrasts with the results reported by Navarro and co-workers for related cyclic ruthenium(II) complexes  $[(\eta^6\text{-}p\text{-cymene})_4\text{Ru}_4(\mu\text{-}4,7\text{-phen-N}^4, \text{N}^7)_2(\mu\text{-OH})_4](\text{NO}_3)_4$  bearing a bridging phenanthroline ligand.<sup>[24]</sup>

Addition of  $\text{TIPF}_6$  to the orange solution containing  $\{[\text{CpRuCl}(\text{PPh}_3)_2(\mu\text{-dppab})]\}$  and the excess of free dppab in  $\text{CH}_2\text{Cl}_2$  led to immediate precipitation of the white  $\text{TiCl}$  powder. After two hours, the decanted supernatant becomes reddish, assuming a fluorescent aspect.

**Crystallographic studies:** To verify whether the proposed solution structures are confirmed in the solid state and also to obtain crystallographic information on this class of compounds, single crystals of **7** and **8** were grown by slow evaporation of a diluted  $\text{C}_2\text{H}_4\text{Cl}_2/\text{EtOH}$  solution. Selected bond lengths and angles for **7** and **8** are provided in Table 1, whereas Table 5 (see the Experimental Section) summarises the main crystallographic data and parameters.

As shown in Figure 3, whereas the asymmetric unit of **7** consists of a single molecule without clathrated solvent mol-

Table 1. Selected bond lengths [ $\text{\AA}$ ] and angles [ $^\circ$ ] for the dinuclear species **7** and **8**.

<b>7</b>		<b>8</b>	
Ru1–P1	2.284(4)	Ru1–P1	2.325(2)
Ru1–P2	2.309(4)	Ru1–P3	2.333(2)
Ru1–Cl1	2.420(5)	Ru1–P2	2.3595(19)
Ru2–P3	2.293(5)		
Ru2–P4	2.270(5)		
Ru2–Cl2	2.444(4)		
P1–Ru1–P2	93.98(14)	P1–Ru1–P3	95.44(7)
P1–Ru1–Cl1	92.2(2)	P1–Ru1–P2	96.98(7)
P2–Ru1–Cl1	96.48(16)	P3–Ru1–P2	94.59(7)
P3–Ru2–P4	93.65(18)		
P3–Ru2–Cl2	95.57(15)		
P4–Ru2–Cl2	91.63(17)		

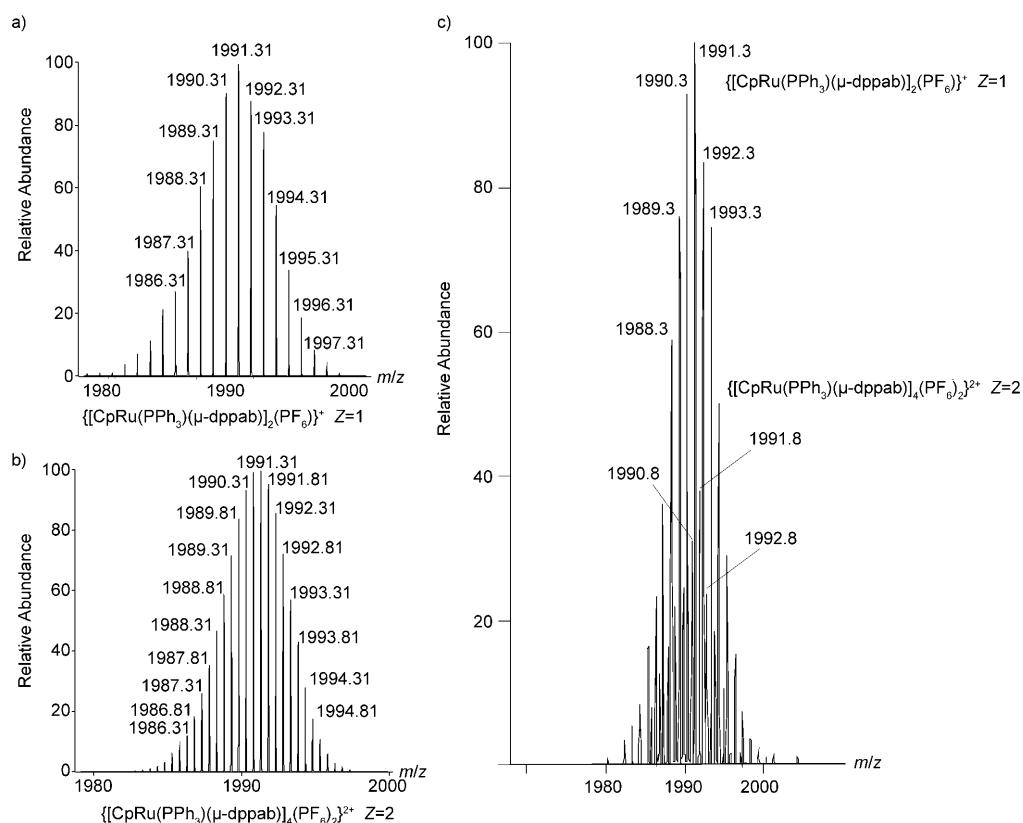


Figure 2. Selected region of the a), b) calculated and c) experimental ESIMS spectra of a solution of **8** and **9** (ca. 1:1 ratio by  $^{31}\text{P}\{^1\text{H}\}$  NMR spectroscopy) and showing the  $[\text{M}-\text{PF}_6]^+$  peak at  $m/z$  1991.3 of the dimetallic complex **8** and the  $[\text{M}-2\text{PF}_6]^{2+}$  peak at  $m/z$  1991.3 of the tetranuclear macrocycle **9**.

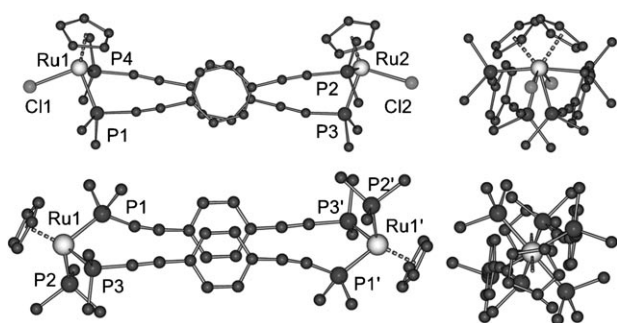


Figure 3. Ball-and-stick diagrams of dimer **7** (top) and **8** (bottom). Two views are shown. On the left, the molecules are perpendicular to the benzene rings of the dppab ligands to show  $\pi$ - $\pi$  stacking. On the right, the complexes are viewed along the metal-metal line. The hydrogen atoms, the carbon atoms of the  $\text{PPh}_3$  ligand (except for the  $\text{C}_{ipso}$ ), the  $\text{PF}_6^-$  anion and the 1,2 dichloroethane solvent molecules are omitted for clarity.

ecules, that of **8** consists of half of the dinuclear dicationic dimer of  $[\{\text{CpRu}(\text{PPh}_3)(\mu, \eta^{1-1}\text{-dppab})\}_2]^{2+}$  together with one  $\text{PF}_6^-$  anion and four 1,2-dichloroethane solvent molecules. In both compounds each ruthenium atom is octahedrally coordinated by two phosphorus atoms belonging to two different dppab ligands in the *cis* position, by the Cp ring in a  $\eta^5$  fashion, thus occupying three contiguous coordination sites, and by a chlorine atom (**7**) or a triphenylphosphine ligand (**8**), respectively. In the neutral complex **7** the ruthenium atoms Ru1 and Ru2 are kept apart by two bridging dppab ligands with a separation between the two metals of 12.74 Å. This distance is shorter than the Ru1–Ru1' distance of 14.83 Å in **8**. Although no related diruthenium compound has been crystallographically authenticated, the intermetallic distance in **7** is comparable to the metal-metal separation found by Manners and co-workers in the related square-planar dipalladium derivatives  $[\{\text{PdI}_2(\text{dppab})\}_2]$  and  $[\{\text{PtI}_2(\text{dppab})\}_2]$  (11.66 and 11.67 Å, respectively).<sup>[25]</sup>

In the diruthenium dication **8**, the Ru–P( $\text{PPh}_3$ ) bond length (Ru1–P2 = 2.3595(19) Å) is slightly longer than the Ru–P(dppab) bond lengths (Ru1–P1 = 2.325(2), Ru1–P3 = 2.333(2) Å). These latter distances are longer than those found in the neutral dimer **7** (Ru1–P1 = 2.284(4), Ru1–P2 = 2.309(4), Ru2–P3 = 2.293(5) and Ru2–P4 = 2.270(5) Å), likely reflecting the presence of two positive charges on the bimetallic moiety. Similarly, the Ru–C<sub>centroid</sub> separations are shorter in **7** (1.863(2), 1.865(2) Å) than in **8** (1.881(3) Å).

The overall shape of the two bimetallic complexes **7** and **8** can be easily compared by looking at Figure 3. Two views, one perpendicular to the central benzene rings and one along the metal-metal direction, are shown.

The central benzene rings of the two dppab molecules are perfectly stacked in an eclipsed conformation in **7**, whereas in **8** they are staggered. The separation between the arene centroids is 3.629(3) Å in **7** and 3.398(2) Å in **8**. In the structurally related Pd and Pt dimers reported by Manners,  $[\{\text{PdI}_2(\text{dppab})\}_2]$  and  $[\{\text{PtI}_2(\text{dppab})\}_2]$ , the phenyl rings of the dppab ligands are largely apart from each other (5.814 and 5.772 Å, respectively).

Dimer **7** (see Figure 3) exhibits a helical arrangement with the two dppab ligands rolled up and slightly stretched; the bridging phenyl rings almost lie one over the other. In dimer **8**, the dppab ligands are parallel to each other, and the bridging phenyl rings are slightly slipped. The same conformation was found in the platinum and palladium dimers.<sup>[25]</sup> Moreover, the two chloride ligands in **7** are mutually rotated ( $\text{Cl1-Ru1-Ru2-Cl2} = -60.7(6)^\circ$ ), whereas in **8** the two terminal  $\text{PPh}_3$  ligands are related by an inversion centre. The overall conformation of **7** is close to that found in  $[\{\text{Cp}^*\text{Mo}_2(\text{dppdfb})\}_2]$ <sup>[26]</sup> ( $\text{Cp}^* = \eta^5\text{-C}_5\text{Me}$ ;  $\text{dppdfb} = \mu^2\text{-1,4-bis(diphenylphosphino)-2,5-difluorobenzene}$ ) with a separation between the aryl centroids of 3.604 Å and a similarly rolled-up disposition of the bridging ligands. The different structures adopted by **7** and **8** is likely due to external supramolecular forces rather than the ligand conformation.<sup>[27]</sup>

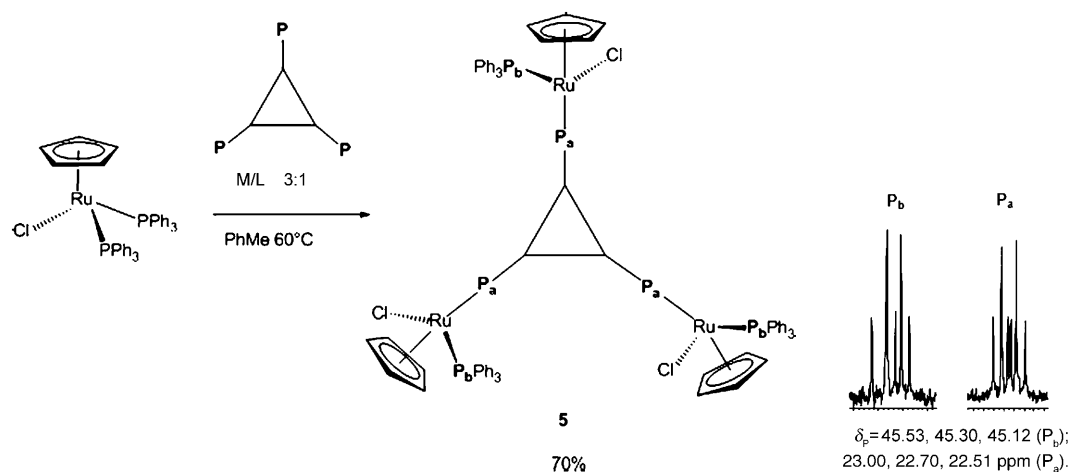
#### Coordination chemistry of tppab towards $[\text{CpRuCl}(\text{PPh}_3)_2]$ :

The coordination chemistry of the tridentate ligand tppab towards  $\{\text{CpRu}\}$  fragments was also briefly investigated. Under the reaction conditions described above, tppab gave the trimetallic species **5** upon reaction of **10** with **2** in a 3:1 M/L ratio in toluene at 60 °C.

The  $^{31}\text{P}\{^1\text{H}\}$  NMR spectrum of **5** disclosed three sets of AM patterns (Scheme 6), which do not correspond to the (two) expected sets of signals deriving from a symmetric system containing a  $\text{C}_3$  axis. This can be explained by the presence of two non-equivalent ligand dispositions around the Ru centres, with concomitant loss of the  $\text{C}_3$  symmetry. If the two stereochemically different Ru atoms are present in a 2:1 ratio, the resulting complex still possesses a symmetry plane, giving three sets of signals on the  $^{31}\text{P}$  NMR spectrum (two diastereoisomers and a *meso* form). To the best of our knowledge, complex **5** is the first example of a ruthenium complex containing three different stereogenic centres with chirality on the metal atom. Although examples of chiral trinuclear metal complexes are known, the chirality in those systems is usually associated with the presence of chiral or atropisomeric ligands.<sup>[28]</sup>

**Electrochemistry and spectroelectrochemistry:** The chloro complexes **10** (mononuclear), **3** and **7** (dinuclear) and **5** (trinuclear) display a substantially similar redox profile in cyclic voltammetry. As a representative example, Figure 4 shows the cyclic voltammetric behaviour of a solution of **3** in dichloromethane.

The dinuclear complex undergoes an oxidation process at  $E^\circ = +0.52$  V, which features chemical and electrochemical reversibility in the time scale of cyclic voltammetry. This first oxidation step is then followed by a further irreversible oxidation almost overlapping the solvent discharge. An irreversible reduction is also present at very negative potential values. Controlled potential coulometry in correspondence to the first anodic process (working potential,  $E_w = +0.9$  V) showed the consumption of two electrons per molecule. As a consequence of the exhaustive oxidation, the original yellow solution turns reddish orange and the resulting solu-



Scheme 6. Synthesis of complex **5**. The related  $^{31}\text{P}\{^1\text{H}\}$  NMR spectroscopic signals are shown on the right side of the scheme.

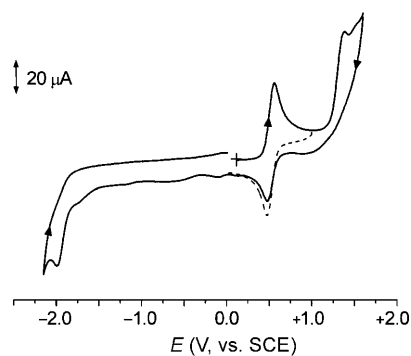


Figure 4. Cyclic voltammogram recorded at a platinum electrode in a solution of **3** in  $\text{CH}_2\text{Cl}_2$  ( $0.8 \times 10^{-3} \text{ mol dm}^{-3}$ ).  $[\text{NBu}_4][\text{PF}_6]$  ( $0.2 \text{ mol dm}^{-3}$ ) supporting electrolyte. Scan rate  $0.2 \text{ V s}^{-1}$ .

tion displays a cyclic voltammetric response quite complementary to the original one, thus confirming the complete stability of the dication  $\mathbf{3}^{2+}$  also over the long times of macroelectrolysis.

As anticipated, the mononuclear **10**, dinuclear **7** and trinuclear **5** compounds display a qualitative similar redox behaviour that results in the electrogeneration of stable cations  $\mathbf{10}^+$ ,  $\mathbf{7}^{2+}$  and  $\mathbf{5}^{3+}$ .

The electrode potentials of the pertinent redox changes are summarised in Table 2. Both first oxidation and reduction steps can be considered metal-based processes. This is also supported by a comparison with the redox behaviour of the benzene ruthenium complexes  $[(\text{C}_6\text{H}_6)\text{RuCl}_2(\text{PR}_3)]$ .<sup>[29]</sup>

Since the oxidation of the two or three  $\text{Ru}^{\text{II}}$  centres present in **3**, **7** and **5**, respectively, occurs in a single step, we can preliminarily assign the respective mixed-valent cations to the charge-localised Robin–Day class I.<sup>[30]</sup> As will be illustrated below, the spectroelectrochemical experiments are in agreement with such an assignment.

As far as the irreversible reduction of **3**, **7** and **5** is concerned, we note that a recent study performed on the relat-

Table 2. Formal electrode potentials (V vs. SCE) and peak-to-peak separations [mV] for the redox changes exhibited by selected dppab and tppab ruthenium complexes in  $\text{CH}_2\text{Cl}_2$ .

	Oxidation processes	Reduction process	
	$E_p^{[a,b]}$	$E_p^{[a,b]}$	
	$E^\circ$	$E_p^{[a,b]}$	
	$\Delta E_p^{[b]}$		
<b>1</b>	+1.4	–	–
<b>10</b>	+1.5	+0.48	–
<b>3</b>	+1.4	+0.52 <sup>[c]</sup>	–2.0
<b>7</b>	+1.5	+0.50 <sup>[c]</sup>	–2.0
<b>5</b>	+1.4	+0.57 <sup>[d]</sup>	–2.0
<b>8</b>	+1.5	+0.50 <sup>[c]</sup>	–1.7

[a] Peak potential value for irreversible processes. [b] Measured at  $0.2 \text{ V s}^{-1}$ . [c] Two-electron process. [d] Three-electron process.

ed complex  $[(\eta^5\text{-ind})\text{RuCl}(\text{PPh}_3)_2]$  (ind = indenyl,  $\text{C}_9\text{H}_7^-$ ) gives evidence that the electrogenerated 19-electron species is unstable and that the chloride atom is rapidly decoordinates.<sup>[31]</sup> Thus, we reasoned that a similar decoordination could take place also in the present case. Finally, a comparison with the redox behaviour of the free dppab ligand **1** suggests that the mentioned irreversible oxidation can be conceivably ascribed to this latter species.

Replacement of the chloride ligand by a  $\text{PPh}_3$  unit to afford complexes **8** and **9** causes severe electrode-poisoning effects in the corresponding electrochemical investigation. Nevertheless, sufficiently defined cyclic voltammograms of **8** have been obtained at a gold electrode and its redox potential values could be assessed. As reported in Table 1, also in this case both the  $\text{Ru}^{\text{II}}/\text{Ru}^{\text{III}}$  electrochemical process and the dppab oxidation appear unaltered with respect to the Cl-containing analogue **7**, whereas the cathodic process moves to a less negative value. The need for repeated electrode cleaning after each cycle prevented further measurements on this compound.

Because of the electrode poisoning, no reliable cyclic voltammogram of the tetramer **9** could be obtained at gold or platinum electrodes, but for the constant appearance of severe adsorption processes around  $-0.5 \text{ V}$ . Due to this fact,

we decided to use an ITO working electrode, which offers a much larger electrode area ( $\text{cm}^2$  versus  $\text{mm}^2$ ) and, as illustrated in Figure 5, the growth of a film was recorded.

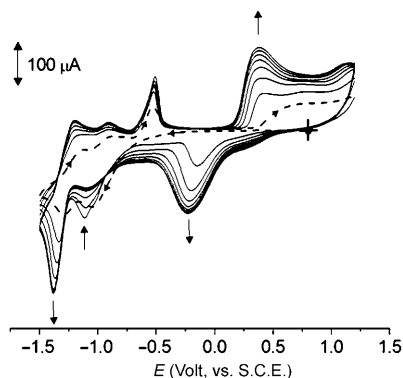


Figure 5. Electrodeposition of a film at an ITO electrode in a solution of **9** in  $\text{CH}_2\text{Cl}_2$  ( $0.1 \times 10^{-3} \text{ mol dm}^{-3}$ ),  $[\text{NBu}_4][\text{PF}_6]$  ( $0.2 \text{ mol dm}^{-3}$ ) supporting electrolyte. Scan rate  $0.05 \text{ V s}^{-1}$ . (-----) Return profile of the first cycle. ● Starting potential.

The observed electrochemical processes show only a minor correspondence with the parent dinuclear compound **8**: in fact, there is an oxidation process with features of electrochemical quasi-reversibility ( $E_{\text{pa}} = +0.38 \text{ V}$ ,  $E_{\text{pc}} = -0.23 \text{ V}$ ), which could correspond to the  $\text{Ru}^{\text{II}}/\text{Ru}^{\text{III}}$  redox change, whereas the reduction at  $-1.4 \text{ V}$ , which triggers the film deposition, corresponds to an unidentified redox process. It is rather common that 19-electron organometallic centres undergo structural reorganisation as a consequence of the loss of one ligand,<sup>[31]</sup> therefore the nature of the film is still unknown and will be the subject of future work.

The spectroelectrochemical analysis in an optically transparent thin-layer electrode (OTTLE) cell allowed us to further confirm the valence-localised nature of the mixed-valent species involved in the electron-transfer processes of **3**, **7** and **5**. Our efforts were directed mainly towards checking for the appearance of an intervalence transition (IT) band that would eventually contrast the Robin–Day classification suggested by cyclic voltammetry. All the UV/Vis spectral data pertaining to the studied complexes are shown in Table 3.

Table 3. Electronic spectral data for complexes **10**, **3**, **7**, **5** and their electrogenerated cations. OTTLE cell,  $\text{THF}/[\text{NBu}_4][\text{PF}_6]$  ( $0.2 \text{ mol dm}^{-3}$ ) solution.

	$\lambda$ [nm]
<b>10</b>	354, 440 <sup>[a]</sup>
<b>10</b> <sup>+</sup>	345, 383, 532, 1250
<b>3</b>	371
<b>3</b> <sup>2+</sup>	388, 550, 1183
<b>7</b>	355
<b>7</b> <sup>+</sup>	378, 535, 1116
<b>5</b>	361
<b>5</b> <sup>3+</sup>	388, 540, 1170

[a] Shoulder.

Irrespective of the investigated species, a general pattern is observed: the spectrum of the neutral complexes is dominated by an intense band in the high-energy region, which can be reasonably ascribed to a metal-to-ligand charge transfer. This band is slightly affected by the oxidation in that, in the spectrum of the cations, two new bands appear at 532–550 (weak) and at 1116–1250 nm (very weak), which can be both ascribed to a  $\text{Ru}^{\text{III}}$  d–d electron transfer. In agreement with the electrochemical results, the UV/Vis spectra of the Cl-containing compounds are also very similar to the mononuclear parent complex **10**, which is in line with the spectral changes observed throughout the oxidation. Remarkably, the spectra of the bi- and trinuclear compounds change monotonically along with the subsequent electron removals. This would support the localised nature of the mixed-valent species. Moreover, no IT band has been detected in the experimental window (low-energy limit = 3300 nm).

In view of the chemical stability of the different electrogenerated cations, we decided to study their magnetic properties by EPR analysis. Since, as discussed above, the different complexes undergo oxidation processes involving a different number of electrons per molecule, in all cases we drew the electrogenerated species after the removal of about 0.7 electrons per molecule.

In agreement with the expected low-spin  $\text{Ru}^{\text{III}}$  species, the absorption pattern is typical of one-electron paramagnetic species, with magnetic features ( $g_i$ ,  $a_i$ ,  $\Delta H_i$ ) characterised by large anisotropies.<sup>[32,33]</sup> The computed lineshape analysis<sup>[34]</sup> can be suitably carried out assuming the following  $S = 1/2$  electron spin Hamiltonian  $H = \beta H g S + \sum_i I_i a_i S$ , which accounts for the actual well-resolved rhombic spectral symmetry ( $\beta H g S =$  electron spin Zeeman interaction between the unpaired electron and the applied magnetic field,  $H$  ( $\beta =$  Bohr magneton,  $g = g$  factor,  $S =$  spin);  $\sum_i I_i a_i S =$  superhyperfine coupling Hamiltonian (shpf) relevant to the sum of the magnetic interactions of the unpaired electron with the different magnetically active nuclei present in the ligand framework ( $I =$  nuclear spin,  $a_i =$  hyperfine splitting)).<sup>[32]</sup> Figure 6 shows the frozen solution spectra ( $\text{CH}_2\text{Cl}_2$ ;  $T = 104 \text{ K}$ ) of complex **7** after controlled-potential one-electron removal.

On the basis of the multiple derivative approach carried out on the experimental spectra and on performing the related computer simulation,<sup>[34]</sup> there is no evidence for hyperfine (hpf) features arising from the naturally occurring  $^{99}\text{Ru}$  ( $I = 5/2$ , natural abundance = 12.8%) and  $^{101}\text{Ru}$  ( $I = 5/2$ , natural abundance = 19.0%).<sup>[32,33]</sup> Such a spectral behaviour is not unusual for glassy solutions of low-spin  $\text{Ru}^{\text{III}}$  compounds, in that they exhibit broad and poorly resolved (first derivative) rhombic lineshapes due to the very low ligand field symmetries experienced by the paramagnetic metal centres.<sup>[32]</sup> As a matter of fact, the spread of the hpf signals of the two magnetically active  $^{99}\text{Ru}$  and  $^{101}\text{Ru}$  nuclei (if any), joined to the effective unpaired electron delocalisation on the ligand framework, does not favour a significant spectral resolution (three largely overlapping anisotropic sextuplets would be expected for the two isotopes of each ruthenium).

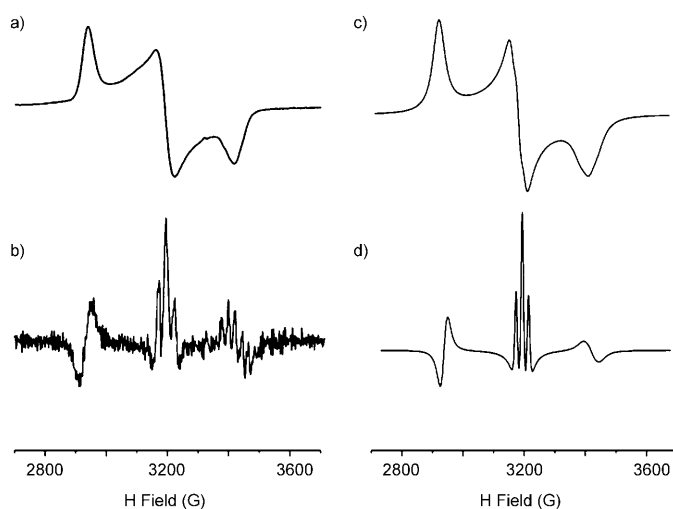


Figure 6. The liquid nitrogen X-band spectrum of **7** after the removal of one electron, in frozen  $\text{CH}_2\text{Cl}_2$ : a) experimental first-derivative spectrum, b) experimental second-derivative spectrum, c) and d) simulated first- and second-derivative spectra, respectively.

nium centre).<sup>[32,33]</sup> Thus, no evidence for magnetic coupling of the unpaired electron with the two naturally occurring  $^{35}\text{Cl}$  ( $I=3/2$ , natural abundance = 75.4%) and  $^{37}\text{Cl}$  ( $I=3/2$ , natural abundance = 24.6%) was detected.

The appearance of the three well-separated absorptions characterised by  $g_i$  values significantly different from that of the free electron ( $g_{\text{electron}}=2.0023$ ) is in agreement with the existence of low-spin  $\text{Ru}^{\text{III}}$  spin-orbit coupling.<sup>[32]</sup> Multiple derivative procedures testify to the presence of two magnetically different phosphine ligands. In fact, the  $g_m$  (m = medium field) lineshape, particularly resolved in the underlying shpf interactions (first- to third-derivative mode), gives evidence of three well-separated signals (theoretical relative intensity 1:2:1) characterised by slightly different linewidths and heights. Such a spectral pattern supports the presence of active  $^{31}\text{P}$  magnetic interactions (second- and third-derivative modes) that arise from the interaction of the unpaired electron with two nearly equivalent P nuclei. By analogy, similar spectral features are expected for the unresolved  $g_l$  and  $g_h$  (l and h = low and high field, respectively) regions, even if the  $g_h$  absorption is affected by the presence of a number of intense spike signals that largely superimpose the underlying phosphorous absorptions (second-derivative mode). Figure 6c and d show the simulated lineshapes, performed on the basis of “mean” shpf  $a(^{31}\text{P})$  values; accordingly, the  $a_l$  and  $a_h$  parameters are evaluated as upper limits for shpf interactions relevant to the corresponding  $\Delta H_i$  as:  $a_l \leq \Delta H_l$ , and  $a_h \leq \Delta H_h$ .

The computed values for whole set of  $S=1/2$  complexes studied here are collected in Table 4.

Upon raising the temperature, the anisotropic signal rapidly reduces before disappearing at the glassy-fluid transition phase ( $T=120$  K). Rapidly refreezing the room-temperature solution makes the rhombic spectrum recover, even if

Table 4. X-band EPR spectra of the studied ruthenium complexes (in  $\text{CH}_2\text{Cl}_2$ ) after one-electron removal, recorded at liquid-nitrogen temperature ( $T=104$  K).<sup>[a]</sup>

	$g_l$	$g_m$	$g_h$	$\langle g \rangle$	$\delta g_{l-h}$	$a_l$	$a_m$	$a_h$	$\langle a \rangle$	$\mu_{\text{eff}}$
<b>10</b>	2.388	2.120	1.949	2.152	0.439	$\leq 29$	32	$\leq 35$	$\leq 32$	1.86
<b>3</b>	2.342	2.124	1.968	2.145	0.374	$\leq 27$	27	$\leq 29$	$\leq 29$	1.86
<b>7</b>	2.302	2.117	1.975	2.131	0.327	$\leq 27$	34	$\leq 36$	$\leq 32$	1.85
<b>5</b>	2.349	2.113	1.963	2.142	0.386	$\leq 28$	25	$\leq 31$	$\leq 28$	1.86

[a]  $g_i$ :  $\pm 0.008$ ;  $a_i$ :  $\pm 1$  G;  $\mu_{\text{eff}}$ :  $\pm 0.01$ ;  $\langle g \rangle = 1/3(g_l + g_m + g_h)$ ;  $\langle a \rangle = 1/3(a_l + a_m + a_h)$ ; l = low field, m = medium field, h = high field;  $\delta g_{l-h} = g_l - g_h$ . For the cations **[3]<sup>+</sup>**, **[7]<sup>+</sup>** and **[6]<sup>+</sup>** the  $a_i$  values refer to mean shpf values (2 nearly magnetically equivalent  $^{31}\text{P}$ ).

it does so with some loss of intensity, which is likely due to the slight instability of the complex upon contact with air.

Such a spectral behaviour holds for all the tested paramagnetic species. On the basis of the anisotropic  $g_i$  features and related  $a_i(^{31}\text{P})$  couplings, the actual singly occupied molecular orbital (SOMO) is expected to be mainly constituted by the 4d  $\text{Ru}^{\text{III}}$  orbitals with important contributions arising from the 3s and 3p orbitals of the two coordinating P atoms.<sup>[32]</sup>

In conclusion, in spite of the different molecular structures of the electrogenerated cations, the X-band multiple derivative approach performed under glassy conditions gives evidence to: 1) the presence of identical rhombic spectral symmetries as supported by similar  $\delta g_{l-h}$  parameters; 2) the significant  $\text{Ru}/^{31}\text{P}$  magnetic interactions in the  $g_m$  and  $g_h$  regions; and 3) the absence of detectable  $\text{Ru}/^{35}\text{Cl}$  and  $\text{Ru}/^{37}\text{Cl}$  magnetic interactions. In keeping with this evidence, the related  $\mu_{\text{eff}}$  parameters are nearly identical and significantly higher than the spin-only value ( $\mu_{\text{eff}} = 1.73 \mu_B$ ), as expected in the presence of effective  $nd$  metal orbital contributions.

## Conclusions

The rigid alkynyldiphosphines dppab and tppab have been synthesised by means of an alternative method that provides better yields and avoids the use of lithium or magnesium salts. The coordination behaviour of the two alkynylphosphines towards the {CpRu} synthon has been investigated using different stoichiometries and reaction conditions that have allowed us to synthesise mononuclear, dinuclear and tetranuclear complexes in which the diphosphine may act as a terminal or bridging ligand between two {CpRu} units. A triruthenium species has been obtained from the tppab ligand.

The presence of stereogenic metal centres in some of these complexes results in the formation of diastereomeric pairs that are easily discernable by NMR spectroscopic methods. Consistently, a rare example of a trinuclear chiral-at-metal complex is generated when the triphosphine tppab is used as a ligand capable of coordinating three {CpRu} moieties. Of particular interest are the two polycations **8** and **9**, which represent intriguing examples of polyruthenamacrocycles that do not interconvert into each other.

The dppab ligands in the dimetallic dimer assume either a parallel conformation or a helical one as shown by the X-ray studies for **7** and **8**, respectively. The central benzene rings of dppab are almost perfectly aligned in **8**, whereas in **7** they are slipped relative to one another. The preference for one shape or the other seems to be imposed by external packing forces in the solid state.

Electrochemistry, supported by spectroelectrochemistry and EPR spectroscopy, pointed out that both dppab and tppab ligands do not allow any efficient communication path between the redox-active Ru centres. In fact, the partially oxidised bi- and trinuclear compounds behave exactly as the parent mononuclear cation [**10**]<sup>+</sup> and can thus be classified as Robin–Day class I mixed-valence complexes with a localised charge.

## Experimental Section

**General:** All manipulations were performed under a dry nitrogen atmosphere using vacuum lines and standard Schlenk techniques. Dichloromethane and methanol were dried by standard methods and distilled under nitrogen before use. All the other solvents were dried and degassed by an MB SPS solvent purification system. 1,4-Diethynylbenzene,<sup>[35]</sup> 1,3,5-triethynylbenzene,<sup>[36]</sup> [CpRu(PPh<sub>3</sub>)<sub>2</sub>Cl]<sup>[37]</sup> and [CpRu(dppe)Cl]<sup>[37]</sup> were prepared from literature methods. Other reagents were obtained from commercial suppliers and used without further purification. Reactions were monitored by TLC on silica gel; detection was made using a KMnO<sub>4</sub> basic solution. Flash column chromatography was performed using glass columns (10–50 mm wide) and silica gel (230–400 mesh).

Deuterated solvents for routine NMR spectroscopic measurements were dried over molecular sieves. <sup>1</sup>H and <sup>13</sup>C[<sup>1</sup>H] NMR spectra were recorded using a Bruker Avance DRX-300 spectrometer operating at 300.13 (<sup>1</sup>H) and 75.48 MHz (<sup>13</sup>C) and a Bruker DRX-400 instrument operating at 400.13 (<sup>1</sup>H) and 100.61 MHz (<sup>13</sup>C). Peak positions are relative to tetramethylsilane (<sup>1</sup>H) and were calibrated against the residual solvent resonance. <sup>31</sup>P[<sup>1</sup>H] NMR spectra were recorded using the same instruments operating at 161.95 and 121.5 MHz. Chemical shifts were measured relative to external 85% H<sub>3</sub>PO<sub>4</sub>, with downfield shifts reported as positive. FTIR spectra were measured using a Perkin–Elmer Spectrum BX instrument with KBr pellets or solution cells. Elemental combustion microanalyses (C, H, N) were obtained using a Perkin–Elmer 2400 series II elemental analyzer.

Mass spectra were obtained at a 70 eV ionisation potential and are reported in the form *m/z* (intensity relative to base = 100). ESIMS spectra were done using an LTQ Orbitrap mass spectrometer (ThermoFisher, San Jose, CA, USA) equipped with a conventional ESI source by direct injection of the sample solution. The instrument parameters were the following: flow rate 3 μl min<sup>-1</sup>, capillary voltage 60 V, tube lens 185 V, nominal resolution (at *m/z* 400) 60000. Eighty scans were accumulated and averaged for each spectrum.

**Electrochemical and spectroelectrochemical studies:** Anhydrous 99.9% dichloromethane was purchased from Aldrich. Fluka [NBu<sub>4</sub>][PF<sub>6</sub>] (electrochemical grade) was used as supporting electrolyte (0.2 mol dm<sup>-3</sup>). Cyclic voltammetry was performed in a three electrode cell containing a platinum working electrode surrounded by a platinum-spiral counter electrode, and an aqueous saturated calomel reference electrode (SCE) mounted with a Luggin capillary. A BAS 100W electrochemical analyzer was used as polarising unit. All the potential values are referred to the saturated calomel electrode (SCE). Under the present experimental conditions, the one-electron oxidation of ferrocene in CH<sub>2</sub>Cl<sub>2</sub> solution occurs at *E*<sup>o</sup> = +0.39 V. Controlled potential coulometry was performed in an H-shaped cell with anodic and cathodic compartments separated by a sintered-glass disk. The working macroelectrode was a platinum gauze; a

mercury pool was used as the counter electrode. The UV/Vis spectroelectrochemical measurements were carried out using a Perkin–Elmer Lambda 900 UV/Vis spectrophotometer and an OTTLE cell equipped with a Pt-minigrid working electrode (32 wires cm<sup>-1</sup>), Pt minigrid auxiliary electrode, Ag wire pseudoreference and CaF<sub>2</sub> windows.<sup>[38]</sup> The electrode potential was controlled during electrolysis by an Amel potentiostat 2059 equipped with an Amel function generator 568. Nitrogen-saturated solutions of the compound under study were used with [NBu<sub>4</sub>][PF<sub>6</sub>] (0.2 mol dm<sup>-3</sup>) as supporting electrolyte. Working potential was kept fixed at the peak potential of the process under study and spectra were progressively collected every 2 min of electrolysis.

X-band EPR spectra were recorded using an ER 200-SRCB Bruker spectrometer. The external magnetic field (*H*) was calibrated using a Microwave Bridge ER041 MR Bruker wavemeter and the temperature was controlled using an ER 4111VT Bruker device (accuracy = ±1 K). The diphenylpicrylhydrazyl (DPPH) free radical was used as suitable “field-marker” (*g*<sub>iso</sub>(DPPH) = 2.0036) for the determination of accurate *g*<sub>i</sub> values. To ensure quantitative spectral reproducibility, the paramagnetic samples were placed into a calibrated quartz capillary tube permanently positioned in the resonance cavity.

**Synthesis of 1,4-bis[(diphenylphosphino)ethynyl]benzene (dppab, **1**):** Chlorodiphenylphosphine (1.8 mL, 9.6 mmol), [Ni(acac)<sub>2</sub>] (0.31 g, 0.12 mmol; acac = acetylacetonate) and Et<sub>3</sub>N (4 mL, 28.8 mmol) were added to a solution of 1,4-diethynylbenzene (0.50 g, 4.0 mmol) in toluene (50 mL). The mixture was stirred at 80 °C for 5 h. The solution was extracted with CH<sub>2</sub>Cl<sub>2</sub> (3 × 40 mL) and the combined organic phases were washed with brine (50 mL), dried over Na<sub>2</sub>SO<sub>4</sub> and concentrated. The crude product was purified by silica gel column chromatography to afford **1** (1.29 g, 65%) as a white, low-melting solid. *R*<sub>f</sub> = 0.6 (*n*-hexane/CH<sub>2</sub>Cl<sub>2</sub> 2:1); <sup>1</sup>H NMR (400 MHz, CDCl<sub>3</sub>, 25 °C): δ = 7.38–7.35 (m, 12H; P-C<sub>6</sub>H<sub>5</sub>), 7.50 (s, 4H; C<sub>6</sub>H<sub>4</sub>), 7.68–7.63 ppm (m, 8H; P-C<sub>6</sub>H<sub>5</sub>); <sup>13</sup>C NMR (100.6 MHz, CDCl<sub>3</sub>, 25 °C): δ = 135.90 (d, <sup>1</sup>*J*(C,P) = 6.3 Hz; P-*ipso*C<sub>6</sub>H<sub>5</sub>), 132.62 (d, <sup>2</sup>*J*(C,P) = 20.7 Hz; P-*ortho*C<sub>6</sub>H<sub>5</sub>), 131.67 (s; C<sub>6</sub>H<sub>4</sub>), 131.65 (s; C<sub>6</sub>H<sub>4</sub>), 129.13 (s; P-*p*C<sub>6</sub>H<sub>5</sub>), 128.67 (d, <sup>3</sup>*J*(C,P) = 7.4 Hz; P-*m*C<sub>6</sub>H<sub>5</sub>), 123.09 (s; *ipso*C<sub>6</sub>H<sub>4</sub>), 107.06 (d, <sup>2</sup>*J*(C,P) = 3.7 Hz; P-C≡), 88.42 ppm (d, <sup>1</sup>*J*(C,P) = 8.1 Hz; ≡ C-C<sub>6</sub>H<sub>5</sub>); <sup>31</sup>P[<sup>1</sup>H] NMR (162.0 MHz, CDCl<sub>3</sub>, 25 °C): δ = -33.3 ppm (s, 2P; P-C<sub>6</sub>H<sub>5</sub>); IR (KBr):  $\tilde{\nu}$  = 2163 cm<sup>-1</sup> (C≡C); MS (70 eV): *m/z* (%): 494 (15) [*M*<sup>+</sup>], 77 (100) [C<sub>6</sub>H<sub>5</sub><sup>+</sup>]; elemental analysis calcd (%) for C<sub>34</sub>H<sub>24</sub>P<sub>2</sub>: C 82.58, H 4.86; found: C 83.01, H 4.55.

**Synthesis of 1,3,5-tris[(diphenylphosphino)ethynyl]benzene (tppab, **2**):** Chlorodiphenylphosphine (2.0 mL, 10.9 mmol), [Ni(acac)<sub>2</sub>] (0.25 g, 0.1 mmol) and Et<sub>3</sub>N (3.3 mL, 23.76 mmol) were added to a solution of 1,3,5-triethynylbenzene (0.50 g, 3.3 mmol) in toluene (50 mL). The mixture was stirred at 80 °C for 5 h. The solution was extracted with CH<sub>2</sub>Cl<sub>2</sub> (3 × 40 mL) and the combined organic phases were washed with brine (50 mL), dried over Na<sub>2</sub>SO<sub>4</sub> and concentrated. The crude product was purified by silica gel column chromatography to afford **2** (1.51 g, 75%) as a white solid. *R*<sub>f</sub> = 0.5 (*n*-hexane/CH<sub>2</sub>Cl<sub>2</sub> 2:1); m.p. 110 °C; <sup>1</sup>H NMR (400 MHz, CDCl<sub>3</sub>, 25 °C): δ = 7.73–7.60 (m, 22H; P-C<sub>6</sub>H<sub>5</sub>), 7.43–7.40 ppm (m, 26H, C<sub>6</sub>H<sub>4</sub>; P-C<sub>6</sub>H<sub>5</sub>); <sup>13</sup>C NMR (100.6 MHz, CDCl<sub>3</sub>, 25 °C): δ = 135.56 (d, <sup>1</sup>*J*(C,P) = 5.9 Hz; P-*ipso*C<sub>6</sub>H<sub>5</sub>), 134.69 (s; C<sub>6</sub>H<sub>4</sub>), 132.69 (d, <sup>2</sup>*J*(C,P) = 21.1 Hz; P-*ortho*C<sub>6</sub>H<sub>5</sub>), 129.16 (s; C<sub>6</sub>H<sub>4</sub>), 128.68 (d, <sup>3</sup>*J*(C,P) = 7.8 Hz; P-*m*C<sub>6</sub>H<sub>5</sub>), 123.56 (s; P-*p*C<sub>6</sub>H<sub>5</sub>), 105.35 (d, <sup>2</sup>*J*(C,P) = 3.0 Hz; P-C≡), 88.22 ppm (d, <sup>1</sup>*J*(C,P) = 10.0 Hz; ≡ C-C<sub>6</sub>H<sub>5</sub>); <sup>31</sup>P[<sup>1</sup>H] NMR (162.0 MHz, CDCl<sub>3</sub>, 25 °C): δ = -33.5 (s, 3P; P-C<sub>6</sub>H<sub>5</sub>); IR (KBr):  $\tilde{\nu}$  = 1577 cm<sup>-1</sup> (C≡C); MS (70 eV): *m/z* (%): 702 (11) [*M*<sup>+</sup>], 77 (100) [C<sub>6</sub>H<sub>5</sub><sup>+</sup>]; elemental analysis calcd (%) for C<sub>48</sub>H<sub>33</sub>P<sub>3</sub>: C 82.04, H 4.73; found: C 81.86, H 4.90.

**Synthesis of [(CpRuCl(PPh<sub>3</sub>)<sub>2</sub>)(μ-dppab)] (**3**):** A solution of dppab (0.68 g, 0.14 mmol) in toluene (10 mL) was added to a solution of [CpRu(PPh<sub>3</sub>)<sub>2</sub>Cl] (0.20 g, 0.28 mmol) in toluene (10 mL). The mixture was stirred at 60 °C for 4 h. The solvent was removed in vacuo, and the residue washed with *n*-hexane at 60 °C, filtered and concentrated under vacuum. The crude product was purified by silica gel column chromatography to afford **3** (0.17 g, 89%) as an orange solid consisting of a 1:1 mixture of two diastereoisomers (NMR spectroscopic signals due to the second diastereoisomer are given in parenthesis). *R*<sub>f</sub> = 0.8 (CH<sub>2</sub>Cl<sub>2</sub>/acetone 20:1); <sup>1</sup>H NMR (400 MHz, CD<sub>2</sub>Cl<sub>2</sub>, 25 °C): δ = 7.95–7.88 (m, 5H), 7.68–7.62 (m, 5H), 7.40–7.33 (m, 9H), 7.26–7.10 (m, 30H), 4.22 (4.23)

ppm (s, 10H);  $^{13}\text{C}$  NMR (100.6 MHz,  $\text{CD}_2\text{Cl}_2$ , 25 °C):  $\delta$  = 140.30 (136.16) (d,  $^1J(\text{C,P})$  = 50.4 Hz; RuP-*ipso*( $\text{C}_6\text{H}_5$ )<sub>2</sub>), 137.07 (d,  $^1J(\text{C,P})$  = 40.4 Hz; RuP-*ipso*( $\text{C}_6\text{H}_5$ )<sub>3</sub>), 134.08 (d,  $^2J(\text{C,P})$  = 10.7 Hz; RuP-*o*( $\text{C}_6\text{H}_5$ )<sub>3</sub>), 132.38 (131.84) (d,  $^3J(\text{C,P})$  = 11.1, 3.0 Hz; RuP-*m*( $\text{C}_6\text{H}_5$ )<sub>2</sub>), 131.90 (s;  $\text{C}_6\text{H}_4$ ), 129.38 (d,  $^4J(\text{C,P})$  = 1.5 Hz; RuP-*p*( $\text{C}_6\text{H}_5$ )<sub>2</sub>), 129.07 (d,  $^4J(\text{C,P})$  = 1.9 Hz; RuP-*p*( $\text{C}_6\text{H}_5$ )<sub>3</sub>), 128.13 (127.99) (d,  $^3J(\text{C,P})$  = 10.2 Hz; RuP-*m*( $\text{C}_6\text{H}_5$ )<sub>3</sub>), 127.49 (d,  $^2J(\text{C,P})$  = 9.6 Hz; RuP-*o*( $\text{C}_6\text{H}_5$ )<sub>2</sub>), 122.97 (122.96) (s; RuP-*ipso*( $\text{C}_6\text{H}_4$ )), 107.34 (d,  $^2J(\text{C,P})$  = 9.3 Hz; PC $\equiv$ C), 89.08 (dd,  $^1J(\text{C,P})$  = 72.4, 2.0 Hz; PC $\equiv$ C), 82.01 (m; Ru- $\text{C}_5\text{H}_5$ );  $^{31}\text{P}\{^1\text{H}\}$  NMR (162.0 MHz,  $\text{CD}_2\text{Cl}_2$ , 25 °C):  $\delta$  = 45.22 (44.94) (d,  $^2J(\text{P,P})$  = 14.1 Hz, 2P; RuP-( $\text{C}_6\text{H}_5$ )<sub>3</sub>), 21.45 (21.17) ppm (d,  $^2J(\text{P,P})$  = 12.8 Hz, 2P; RuP-( $\text{C}_6\text{H}_5$ )<sub>2</sub>); IR (KBr):  $\tilde{\nu}$  = 2166 (C $\equiv$ C), 1720, 802  $\text{cm}^{-1}$ ; ESIMS (MeOH) positive ion:  $m/z$  (%): 1422 (21) [ $\text{M}^+$ ], 1387 (20) [ $\text{M}^+ - \text{Cl}$ ], 673 (100) [ $\text{CpRuCl}(\text{PPh}_3)(\text{Ph}_2\text{P}-\text{C}\equiv\text{C})^+$ ]; elemental analysis calcd (%) for  $\text{C}_{80}\text{H}_{64}\text{Cl}_2\text{P}_4\text{Ru}_2$ : C 67.56, H 4.54; found: C 66.36, H 4.11.

**Synthesis of [(CpRu(dppe))<sub>2</sub>(μ-dppab)](PF<sub>6</sub>)<sub>2</sub> (4):** A solution of TlPF<sub>6</sub> (0.13 g, 0.37 mmol) in MeOH (0.5 mL) was added to a solution of [CpRu(dppe)Cl] (0.10 g, 0.17 mmol) in dichloromethane (30 mL). The mixture was stirred for 4 h and the supernatant was separated from TlCl. A solution of dppab (0.04 g, 0.08 mmol) in dichloromethane (10 mL) was then mixed together with the previous solution and stirred at room temperature overnight. After this time, the solvent was removed in vacuo, and the solid residue washed with warm *n*-hexane (2 × 20 mL at 60 °C) and dried under vacuum. The crude product was purified by silica gel column chromatography to afford **4** (0.10 g, 65 %) as an orange solid.  $R_f$  = 0.3 ( $\text{CH}_2\text{Cl}_2/\text{acetone}$  20:1);  $^1\text{H}$  NMR (400 MHz,  $\text{CD}_2\text{Cl}_2$ , 25 °C):  $\delta$  = 7.68 (m, 4H), 7.47–7.17 (m, 60H), 6.96–6.89 (m, 8H), 4.99 (s, 10H), 3.21–3.15 (m, 4H), 2.71–2.73 (m, 4H);  $^{13}\text{C}$  NMR (100.6 MHz,  $\text{CD}_2\text{Cl}_2$ , 25 °C):  $\delta$  = 135.34 (m; RuP-*ipso*( $\text{C}_6\text{H}_5$ )<sub>2</sub>), 134.77 (m; RuP-*ipso*( $\text{C}_6\text{H}_5$ )dppab), 133.22 (s;  $\text{C}_6\text{H}_4$ ), 131.78–131.68 (m; RuP-*m*( $\text{C}_6\text{H}_5$ )dppab), 131.53–131.43 (m; RuP-*m*( $\text{C}_6\text{H}_5$ )dppab), 131.27 (m,  $^2J(\text{C,P})$  = 12.6 Hz; RuP-*o*( $\text{C}_6\text{H}_5$ )dppab), 130.52 (m,  $^2J(\text{C,P})$  = 12.6 Hz; RuP-*o*( $\text{C}_6\text{H}_5$ )dppab), 130.07 (brs; RuP-*p*( $\text{C}_6\text{H}_5$ )<sub>2</sub>), 128.84–128.66 (m; RuP-*m*( $\text{C}_6\text{H}_5$ )<sub>2</sub> + RuP-*p*( $\text{C}_6\text{H}_5$ )dppab), 128.41 (d,  $^2J(\text{C,P})$  = 11.1 Hz; RuP-*o*( $\text{C}_6\text{H}_5$ )<sub>2</sub>), 122.33 (d,  $^3J(\text{C,P})$  = 2.2 Hz; RuP-*ipso*( $\text{C}_6\text{H}_4$ )), 106.58–106.44 (m; RuPC $\equiv$ C), 88.34–87.60 (m; RuPC $\equiv$ C), 86.22 ppm (m; Ru- $\text{C}_5\text{H}_5$ ), 26.70 ppm (dm,  $^1J(\text{P,P})$  = 23.7 Hz; RuP- $\text{CH}_2$ ) 26.48 (dm,  $^1J(\text{P,P})$  = 22.2 Hz; RuP- $\text{CH}_2$ );  $^{31}\text{P}\{^1\text{H}\}$  NMR (162.0 MHz,  $\text{CD}_2\text{Cl}_2$ , 25 °C):  $\delta$  = 70.99 (d,  $^2J(\text{P,P})$  = 36.5 Hz, 1P; RuP-( $\text{C}_6\text{H}_5$ )<sub>2</sub>), 30.33 (t,  $^2J(\text{P,P})$  = 36.5 Hz, 2P; RuP-( $\text{C}_6\text{H}_5$ )<sub>2</sub>), –144.4 ppm (sept,  $^1J(\text{P,P})$  = 711.2 Hz, 2P, PF<sub>6</sub>); IR (KBr):  $\tilde{\nu}$  = 2171 (C $\equiv$ C), 840  $\text{cm}^{-1}$  (P-F); ESIMS (MeOH) positive ion:  $m/z$  (%): 1796 (19) [ $\text{M} - \text{PF}_6$ ] $^+$ ; elemental analysis calcd (%) for  $\text{C}_{96}\text{H}_{82}\text{F}_{12}\text{P}_8\text{Ru}_2$ : C 60.25, H 4.32; found: C 60.46, H 4.70.

**Synthesis of [(CpRuCl(PPh<sub>3</sub>)<sub>3</sub>)(μ<sub>3</sub>-tppab)] (5):** A solution of tppab (0.15 g, 0.20 mmol) in toluene (35 mL) was added to a solution of [CpRu(PPh<sub>3</sub>)<sub>2</sub>Cl] (0.47 g, 0.60 mmol) in the same solvent (30 mL). The mixture was stirred at 60 °C for 3 h. The solvent was removed in vacuo, and the solid residue washed with warm hexane (2 × 20 mL at 60 °C) and dried under vacuum. The crude product was purified by silica gel column chromatography to afford **5** (0.30 g, 70 %) as an orange solid containing a 1.2:1 mixture of three diastereoisomers ( $^{31}\text{P}$  NMR spectroscopic signals of diastereoisomers are given in parenthesis).  $R_f$  = 0.6 ( $\text{CH}_2\text{Cl}_2/\text{acetone}$  30:1);  $^1\text{H}$  NMR (400 MHz,  $\text{CD}_2\text{Cl}_2$ , 25 °C):  $\delta$  = 7.86–7.76 (m, 8H), 7.71–7.61 (m, 8H), 7.38–7.03 (m, 62H), 4.22 ppm (s, 15H);  $^{13}\text{C}$  NMR (100.6 MHz,  $\text{CD}_2\text{Cl}_2$ , 25 °C):  $\delta$  = 139.95 (135.91) (d,  $^1J(\text{C,P})$  = 46.5 Hz; RuP-*ipso*( $\text{C}_6\text{H}_5$ )<sub>2</sub>), 136.91 (d,  $^1J(\text{C,P})$  = 40.7 Hz; RuP-*ipso*( $\text{C}_6\text{H}_5$ )<sub>3</sub>), 134.04 (d,  $^2J(\text{C,P})$  = 10.7 Hz; RuP-*o*( $\text{C}_6\text{H}_5$ )<sub>3</sub>), 132.60–132.36 (132.82–131.59) (m; RuP-*m*( $\text{C}_6\text{H}_5$ )<sub>2</sub>), 129.45 (brs, 3C;  $\text{C}_6\text{H}_3$ ), 129.26 (brs; RuP-*p*( $\text{C}_6\text{H}_5$ )<sub>2</sub>), 129.12 (brs; RuP-*p*( $\text{C}_6\text{H}_5$ )<sub>3</sub>), 128.17 (127.99) (d,  $^3J(\text{C,P})$  = 10.0 Hz; RuP-*m*( $\text{C}_6\text{H}_5$ )<sub>3</sub>), 127.48 (d,  $^2J(\text{C,P})$  = 9.3 Hz; RuP-*o*( $\text{C}_6\text{H}_5$ )<sub>2</sub>), 122.82 (brs; RuP-*ipso*( $\text{C}_6\text{H}_4$ )<sub>3</sub>), 105.11 (d,  $^2J(\text{C,P})$  = 8.9 Hz; RuPC $\equiv$ C), 88.83 (brd,  $^1J(\text{C,P})$  = 68.1 Hz; RuPC $\equiv$ C), 82.00 ppm (m; Ru- $\text{C}_5\text{H}_5$ );  $^{31}\text{P}\{^1\text{H}\}$  NMR (162.0 MHz,  $\text{CD}_2\text{Cl}_2$ , 25 °C):  $\delta$  = 45.53 (45.30, 45.129) (d,  $^2J(\text{P,P})$  = 46.7 Hz, 3P; RuP-( $\text{C}_6\text{H}_5$ )<sub>3</sub>), 23.00 (22.70, 22.51) (d,  $^2J(\text{P,P})$  = 46.7 Hz, 3P; RuP-( $\text{C}_6\text{H}_5$ )<sub>2</sub>); IR (KBr):  $\tilde{\nu}$  = 2175 (C $\equiv$ C), 840  $\text{cm}^{-1}$  (P-F); ESIMS (MeOH) positive ion:  $m/z$  (%): 673 (17) [ $\text{M} - \text{C}_6\text{H}_5 - (\text{CpRuCl}(\text{PPh}_3)_3 - \text{C}\equiv\text{C})^+$ ], 2059 (100) [ $\text{M} - \text{Cl}$ ] $^+$ , 2094 (15) [ $\text{M}^+$ ] $^+$ ; elemental analysis calcd (%) for  $\text{C}_{117}\text{H}_{95}\text{Cl}_3\text{P}_6\text{Ru}_3$ : C 67.10, H 4.48; found: C 66.86, H 4.91.

**Synthesis of [CpRuCl(η<sup>1</sup>-dppab)] (6):** A solution of **1** (0.15 g, 0.30 mmol) in toluene (10 mL) was added to a solution of [CpRu(PPh<sub>3</sub>)<sub>2</sub>Cl] (**10**) (0.11 g, 0.15 mmol) in toluene (10 mL). The mixture was stirred at 60 °C for 1 h. The solvent was removed in vacuo, and the solid residue washed with warm *n*-hexane (2 × 20 mL) and dried under vacuum. The crude product was purified by silica gel column chromatography to afford **6** (0.31 g, 22 %) as a yellow solid.  $R_f$  = 0.7 ( $\text{CH}_2\text{Cl}_2/\text{acetone}$  20:1);  $^1\text{H}$  NMR (400 MHz,  $\text{CD}_2\text{Cl}_2$ , 25 °C):  $\delta$  = 7.97–7.91 (m, 2H), 7.69–7.50 (m, 8H), 7.39–7.29 (m, 17H), 7.23–7.17 (m, 4H), 7.13–7.06 (m, 8H), 4.23 ppm (s, 5H,  $\text{C}_5\text{H}_5$ );  $^{13}\text{C}$  NMR (100.6 MHz,  $\text{CD}_2\text{Cl}_2$ , 25 °C):  $\delta$  = 140.58 (dd,  $J(\text{C,P})$  = 50.0, 3.3 Hz; RuP-*ipso*( $\text{C}_6\text{H}_5$ )<sub>2</sub>), 137.02 (dd,  $J(\text{C,P})$  = 4 0.6, 1.7 Hz; RuP-*ipso*( $\text{C}_6\text{H}_5$ )<sub>3</sub>), 135.99 (d,  $^1J(\text{C,P})$  = 42.2 Hz;  $\equiv$ C-*ipso*P( $\text{C}_6\text{H}_5$ )<sub>2</sub>), 135.98 (d,  $^3J(\text{C,P})$  = 6.7 Hz; RuP-*m*( $\text{C}_6\text{H}_5$ )<sub>2</sub>), 134.03 (d,  $^2J(\text{C,P})$  = 10.7 Hz; RuP-*o*( $\text{C}_6\text{H}_5$ )<sub>3</sub>), 132.73 (s;  $\text{C}_6\text{H}_4$ ), 132.52 (s;  $\text{C}_6\text{H}_4$ ), 131.94 (d,  $^4J(\text{C,P})$  = 1.1 Hz; RuP-*p*( $\text{C}_6\text{H}_5$ )<sub>2</sub>), 131.71 (d,  $^4J(\text{C,P})$  = 1.5 Hz;  $\equiv$ C-P( $\text{C}_6\text{H}_5$ )<sub>2</sub>), 129.05 (d,  $^4J(\text{C,P})$  = 1.85 Hz; RuP-*p*( $\text{C}_6\text{H}_5$ )<sub>3</sub>), 128.81 (d,  $^2J(\text{C,P})$  = 7.4 Hz; RuP-*p*( $\text{C}_6\text{H}_5$ )<sub>2</sub>), 128.79 (s;  $\text{C}_6\text{H}_4$ ), 128.08 (d,  $^3J(\text{C,P})$  = 10.0 Hz; RuP-*m*( $\text{C}_6\text{H}_5$ )<sub>3</sub>), 127.91 (d,  $^3J(\text{C,P})$  = 10.0 Hz; RuP-*m*( $\text{C}_6\text{H}_5$ )<sub>2</sub>), 127.47 (d,  $^2J(\text{C,P})$  = 9.6 Hz;  $\equiv$ C-P( $\text{C}_6\text{H}_5$ )<sub>2</sub>), 123.60 (d,  $^3J(\text{C,P})$  = 1.5 Hz;  $\text{C}_6\text{H}_4$ ), 122.50 (d,  $^1J(\text{C,P})$  = 2.2 Hz; RuPC $\equiv$ C), 107.40 (d,  $^2J(\text{C,P})$  = 10.0 Hz; RuPC $\equiv$ C), 107.06 (d,  $^1J(\text{C,P})$  = 10.0 Hz;  $\equiv$ C-P( $\text{C}_6\text{H}_5$ )<sub>2</sub>), 88.83 (d,  $^1J(\text{C,P})$  = 9.6 Hz; C $\equiv$ C-P( $\text{C}_6\text{H}_5$ )<sub>2</sub>), 82.00 ppm (m; Ru- $\text{C}_5\text{H}_5$ );  $^{31}\text{P}\{^1\text{H}\}$  NMR (400 MHz,  $\text{CD}_2\text{Cl}_2$ , 25 °C):  $\delta$  = 44.99 (d,  $^2J(\text{P,P})$  = 45.9 Hz, 1P; RuP-( $\text{C}_6\text{H}_5$ )<sub>3</sub>),  $\delta$  = 20.24 ( $^2J(\text{P,P})$  = 45.9 Hz, 1P; RuP-( $\text{C}_6\text{H}_5$ )<sub>2</sub>), –33.64 ppm (s, 1P;  $\equiv$ C-P( $\text{C}_6\text{H}_5$ )<sub>2</sub>); IR (KBr):  $\tilde{\nu}$  = 2172  $\text{cm}^{-1}$  (C $\equiv$ C); ESIMS (MeOH) positive ion:  $m/z$  (%): 958 (12) [ $\text{M}^+$ ] $^+$ ; elemental analysis calcd (%) for  $\text{C}_{57}\text{H}_{44}\text{ClP}_3\text{Ru}$ : C 71.43, H 4.63; found: C 72.31, H 4.75.

**Synthesis of [(CpRuCl)(μ-dppab)]<sub>2</sub> (7):** A solution of dppab (0.68 g, 0.40 mmol) in toluene (10 mL) was added to a solution of [CpRu(PPh<sub>3</sub>)<sub>2</sub>Cl] (0.15 g, 0.20 mmol) in toluene (20 mL). The mixture was gently brought to reflux and stirred for 4 h. After this time, the supernatant was filtered off and the solid residue washed with warm *n*-hexane (2 × 20 mL at 60 °C) and dried under vacuum. The crude product was purified by silica gel column chromatography to afford **7** (0.67 g, 25 %) as an orange solid.  $R_f$  = 0.8 ( $\text{CH}_2\text{Cl}_2/\text{acetone}$  20:1);  $^1\text{H}$  NMR (400 MHz,  $\text{CD}_2\text{Cl}_2$ , 25 °C):  $\delta$  = 8.18–8.13 (m, 8H), 7.58–7.53 (m, 8H), 7.39–7.32 (m, 12H), 7.21 (s, 8H), 7.00–6.96 (m, 4H), 6.89–6.86 (m, 8H), 4.49 ppm (s, 10H);  $^{13}\text{C}$  NMR (100.6 MHz,  $\text{CD}_2\text{Cl}_2$ , 25 °C):  $\delta$  = 140.41 (m; RuP-*ipso*( $\text{C}_6\text{H}_5$ )<sub>2</sub>), 135.24 (m; RuP-*ipso*( $\text{C}_6\text{H}_5$ )<sub>2</sub>), 131.87 (m; RuP-*o*( $\text{C}_6\text{H}_5$ )<sub>2</sub>), 131.46 (m; RuP-*o*( $\text{C}_6\text{H}_5$ )<sub>2</sub> +  $\text{C}_6\text{H}_4$ ), 129.49 (s; RuP-*p*( $\text{C}_6\text{H}_5$ )<sub>2</sub>), 128.70 (s; RuP-*p*( $\text{C}_6\text{H}_5$ )<sub>2</sub>), 128.07 (m; RuP-*m*( $\text{C}_6\text{H}_5$ )<sub>2</sub>), 127.54 (m; RuP-*m*( $\text{C}_6\text{H}_5$ )<sub>2</sub>), 122.60 (s;  $\text{C}_6\text{H}_4$ ), 107.82 (m; RuPC $\equiv$ C), 86.74 (m; RuPC $\equiv$ C), 83.29 ppm (s; Ru- $\text{C}_5\text{H}_5$ );  $^{31}\text{P}\{^1\text{H}\}$  NMR (162.0 MHz,  $\text{CD}_2\text{Cl}_2$ , 25 °C):  $\delta$  = 18.67 ppm (s, 4P; P-( $\text{C}_6\text{H}_5$ )<sub>2</sub>); IR (KBr):  $\tilde{\nu}$  = 2172  $\text{cm}^{-1}$  (C $\equiv$ C); ESIMS (MeOH) positive ion:  $m/z$  (%): 1359 (20) [ $\text{M} - \text{Cl}$ ] $^+$ , 1392 (35) [ $\text{M}^+$ ] $^+$ ; elemental analysis calcd (%) for  $\text{C}_{78}\text{H}_{58}\text{Cl}_2\text{P}_4\text{Ru}_2$ : C 67.29, H 4.20; found: C 66.95, H 4.70.

**Synthesis of [(CpRu(PPh<sub>3</sub>)(μ-dppab)]<sub>2</sub>(PF<sub>6</sub>)<sub>2</sub> (8) and [(CpRu(PPh<sub>3</sub>)(μ-dppab)]<sub>4</sub>(PF<sub>6</sub>)<sub>4</sub> (9):** A solution of TlPF<sub>6</sub> (0.40 g, 0.15 mmol) in MeOH (0.5 mL) was added to a solution of **3** (0.74 g, 0.52 mmol) and dppab (0.26 g, 0.52 mmol) in dichloromethane (30 mL). The mixture was stirred for 2 h and the supernatant was separated from TlCl by filtration. After this time, the solvent was removed in vacuo and the solid residue dried. The crude product was purified by silica gel column chromatography (dichloromethane/acetone 20:1) to afford an orange solid (0.87 g, 57 % based on **3**) consisting of a mixture of **8** and **9** in an approximate 1:1 ratio. Dissolution of the solid mixture in ca. 150 mL  $\text{CH}_2\text{Cl}_2$ , followed by slow addition of *n*-hexane, led to selective precipitation of **9** (0.47 g, 21 % based on **3**) as a yellow solid. The remaining red solution was concentrated to dryness to afford pure **8** (0.40 g, 36 % based on **3**).

**Compound 8:**  $R_f$  = 0.6 ( $\text{CH}_2\text{Cl}_2/\text{acetone}$  20:1);  $^1\text{H}$  NMR (400 MHz,  $\text{CD}_2\text{Cl}_2$ , 25 °C):  $\delta$  = 7.70–7.47 (m, 40H), 7.37–7.11 (m, 30H), 7.03 (s, 8H), 4.83 ppm (s, 10H);  $^{13}\text{C}$  NMR (100.6 MHz,  $\text{CD}_2\text{Cl}_2$ , 25 °C):  $\delta$  = 135.95–135.23 (m; RuP-*ipso*( $\text{C}_6\text{H}_5$ )<sub>3</sub> + RuP-*ipso*( $\text{C}_6\text{H}_5$ )<sub>2</sub>), 133.54 (d,  $^2J(\text{C,P})$  = 10.4 Hz; RuP-*o*( $\text{C}_6\text{H}_5$ )<sub>3</sub>), 132.01–131.91 (m; RuP-*o*( $\text{C}_6\text{H}_5$ )<sub>2</sub>), 131.70 (brs;  $\text{C}_6\text{H}_4$ ), 131.11–130.56 (m; RuP-*m*( $\text{C}_6\text{H}_5$ )<sub>2</sub>), 130.20 (brs; RuP-*p*( $\text{C}_6\text{H}_5$ )<sub>3</sub>), 128.83–128.35 (m; RuP-*p*( $\text{C}_6\text{H}_5$ )<sub>2</sub> + RuP-*m*( $\text{C}_6\text{H}_5$ )<sub>3</sub>), 122.16 (s; RuP-*ipso*( $\text{C}_6\text{H}_4$ )<sub>3</sub>), 108.27–108.17 (m; RuPC $\equiv$ C), 87.92 (d,  $^1J(\text{C,P})$  = 79.1 Hz; RuPC $\equiv$ C), 86.18 ppm (m; Ru- $\text{C}_5\text{H}_5$ );  $^{31}\text{P}\{^1\text{H}\}$  NMR (162.0 MHz,  $\text{CD}_2\text{Cl}_2$ ,

25°C):  $\delta$  = 38.95 (t,  $^2J(\text{P,P})$  = 37.5 Hz, 4P; RuP-(C<sub>6</sub>H<sub>5</sub>)<sub>2</sub>), 20.26 (d,  $^2J(\text{P,P})$  = 37.5 Hz, 2P; RuP-(C<sub>6</sub>H<sub>5</sub>)<sub>2</sub>), -144.6 ppm (sept,  $^1J(\text{P,F})$  = 706.3 Hz, 2P; PF<sub>6</sub>); IR (KBr):  $\tilde{\nu}$  = 2168 (C≡C), 837 cm<sup>-1</sup> (P-F); ESIMS (MeOH) positive ion:  $m/z$  (%): 1991 (100) [M-PF<sub>6</sub>]<sup>+</sup>; elemental analysis calcd (%) for C<sub>114</sub>H<sub>88</sub>F<sub>12</sub>P<sub>8</sub>Ru<sub>2</sub>: C 64.11, H 4.15; found: C 64.36, H 4.98.

**Compound 9:**  $R_f$  = 0.4 (CH<sub>2</sub>Cl<sub>2</sub>/acetone 20:1); <sup>1</sup>H NMR (400 MHz, CD<sub>2</sub>Cl<sub>2</sub>, 25°C):  $\delta$  = 7.72–7.67 (m, 20H), 7.53–7.43 (m, 60H), 7.28–7.20 (m, 60H), 7.08 (brs, 16H), 4.84 ppm (s, 20H); <sup>13</sup>C NMR (100.6 MHz, CD<sub>2</sub>Cl<sub>2</sub>, 25°C):  $\delta$  = 137.45–136.64 (m; RuP-*ipso*(C<sub>6</sub>H<sub>5</sub>)) + RuP-*ipso*(C<sub>6</sub>H<sub>5</sub>)<sub>2</sub>), 133.59 (d,  $^2J(\text{C,P})$  = 10.4 Hz; RuP-*o*(C<sub>6</sub>H<sub>5</sub>)<sub>3</sub>), 133.05–132.92 (m; RuP-*o*(C<sub>6</sub>H<sub>5</sub>)<sub>2</sub>), 132.09–131.97 (m; RuP-*o*(C<sub>6</sub>H<sub>5</sub>)<sub>2</sub>), 131.84 (brs; C<sub>6</sub>H<sub>5</sub>), 131.81–130.83 (m; RuP-*m*(C<sub>6</sub>H<sub>5</sub>)<sub>2</sub>), 129.71 (brs; RuP-*p*(C<sub>6</sub>H<sub>5</sub>)<sub>3</sub>), 128.91–128.40 (m; RuP-*p*(C<sub>6</sub>H<sub>5</sub>)<sub>2</sub> + RuP-*m*(C<sub>6</sub>H<sub>5</sub>)<sub>3</sub>), 122.17 (s; RuP-*ipso*(C<sub>6</sub>H<sub>5</sub>)), 107.34–107.25 (m; RuPC≡C), 87.92 (d,  $^1J(\text{C,P})$  = 80.4 Hz; RuPC≡), 86.22 ppm (m; Ru-C<sub>3</sub>H<sub>5</sub>); <sup>31</sup>P{<sup>1</sup>H} NMR (162.0 MHz, CD<sub>2</sub>Cl<sub>2</sub>, 25°C):  $\delta$  = 39.23 (t,  $^2J(\text{P,P})$  = 38.5 Hz; 8P, RuP-(C<sub>6</sub>H<sub>5</sub>)<sub>2</sub>), 23.88 (d,  $^2J(\text{P,P})$  = 38.5 Hz, 4P, RuP-(C<sub>6</sub>H<sub>5</sub>)<sub>2</sub>), -144.6 (sept,  $^1J(\text{P,F})$  = 706.3 Hz, 4P; PF<sub>6</sub>); IR (KBr):  $\tilde{\nu}$  = 2168 (C≡C), 837 cm<sup>-1</sup> (P-F); ESIMS (MeOH) positive ion:  $m/z$  (%): 923 (100) [Cp<sub>2</sub>Ru<sub>2</sub>(PPH<sub>3</sub>)<sub>2</sub> (dppab)]<sup>2+</sup>, 1991 (5) [M-2PF<sub>6</sub>]<sup>2+</sup>; elemental analysis calcd (%) for C<sub>228</sub>H<sub>176</sub>F<sub>24</sub>P<sub>16</sub>Ru<sub>4</sub>: C 64.11, H 4.15; found: C 64.23, H 4.21.

**Crystallographic studies:** Data collection for complexes **7** and **8** was carried out using an Oxford Diffraction Xcalibur3 diffractometer equipped with MoK $\alpha$  radiation (0.71073 Å). Data collection was performed at 150 K with the program CrysAlis CCD<sup>[39]</sup> and data reduction was carried out

with the program CrysAlis RED<sup>[40]</sup>. Absorption correction was applied through the program ABSPACK<sup>[40]</sup>. The structures were solved with direct methods implemented in the program Sir97<sup>[41]</sup> and the refinement was completed by full-matrix least squares against  $F^2$  using all data implemented in SHELXL<sup>[42]</sup>. Full details of crystallographic data are given in Table 5.

In compound **7**, a merohedral twinning is present and the twin component was found to be 0.50(7). The cyclopentadienyl ring bonded to Ru2 was fitted as a rigid group and the carbon atoms were restrained to have the same U<sub>ij</sub> components. All the non-hydrogen atoms were refined anisotropically and the hydrogen atoms were fixed in calculated positions and refined isotropically with thermal factors related to those of the atom they are bound to.

The crystals of **8** were unstable when removed from the mother liquor at room temperature and they were mounted using cryo-techniques. All the non-hydrogen atoms were refined anisotropically, except for the carbon atoms of three solvent molecules of 1,2-dichloroethane. The C–C and the C–Cl bond lengths of the latter were restrained to 1.55 Å and forced to be equal with an estimated standard deviation of 0.02. The hydrogen atoms were placed in calculated positions and refined isotropically with thermal factors related to those of the atom they are bound to. Geometrical calculations were performed by PARST97<sup>[43]</sup> and molecular plots were produced by the program ORTEP3<sup>[44]</sup>. All the calculations were performed using the package WINGX<sup>[45]</sup>.

Table 5. Crystal data and structure refinement for compounds **7** and **8**.

	<b>7</b>	<b>8</b>
formula	C <sub>78</sub> H <sub>58</sub> Cl <sub>2</sub> P <sub>4</sub> Ru <sub>2</sub>	C <sub>130</sub> H <sub>120</sub> Cl <sub>16</sub> F <sub>12</sub> P <sub>8</sub> Ru <sub>2</sub>
$M_r$	1392.16	2927.36
$T$ [K]	150(2)	150(2)
$\lambda$ [Å]	0.71069	0.71069
crystal system	orthorhombic	triclinic
space group	$Pca2_1$	$\bar{P}1$
$a$ [Å]	18.7930(10)	12.7488(5)
$b$ [Å]	17.3350(10)	15.2991(8)
$c$ [Å]	20.0080(10)	19.4914(9)
$\alpha$ [°]	90	67.404(5)
$\beta$ [°]	90	74.656(4)
$\gamma$ [°]	90	83.577(4)
$V$ [Å <sup>3</sup> ]	6518.1(6)	3384.5(3)
$Z$	4	1
$\rho_{\text{calcd}}$ [Mg m <sup>-3</sup> ]	1.419	1.436
$\mu$ [mm <sup>-1</sup> ]	0.688	0.697
$F(000)$	2832	1488
size [mm <sup>3</sup> ]	0.15 × 0.07 × 0.05	0.2 × 0.15 × 0.1
$\theta$ range [°]	3.75 to 25.00	3.73 to 27.49
limiting indices	-22 ≤ $h$ ≤ 15, -20 ≤ $k$ ≤ 20, -23 ≤ $l$ ≤ 23	-15 ≤ $h$ ≤ 15, -18 ≤ $k$ ≤ 19, -25 ≤ $l$ ≤ 23
reflns collected	23 772	22 066
unique reflns	10 001	12 383
$R_{\text{int}}$	0.0907	0.0431
completeness to $\theta = 25^\circ$ [%]	99.2	96.4
absorption correction	semi-empirical from equivalents	semi-empirical from equivalents
max/min transmission	0.9662/0.9271	1/0.76941
data/restraints/parameters	10 001/1/771	12 383/9/727
goodness-of-fit on $F^2$	0.926	1.061
final $R$ indices ( $I > 2\sigma(I)$ )	$R_1 = 0.0774$ , $wR_2 = 0.1661$	$R_1 = 0.0978$ , $wR_2 = 0.2762$
$R$ indices (all data)	$R_1 = 0.1639$ , $wR_2 = 0.2194$	$R_1 = 0.1393$ , $wR_2 = 0.3073$
absolute structure parameter	0.52(7)	-
largest diff. peak and hole [e Å <sup>-3</sup> ]	0.960 and -0.669	2.184 and -1.121

## Acknowledgements

B.D.C., A.R. and M.P. acknowledge the motu proprio FIRENZE HYDROLAB project by Ente Cassa di Risparmio di Firenze (<http://www.iccom.cnr.it/hydrolab/>) and PRIN 2007 (MIUR) for funding this research activity, through a doctoral grant to B.D.C. and a post-doctoral grant to A.R. B.D.C. would like to thank Mr. Fabrizio Zanobini for experimental support at ICCOM-CNR, and Dr. Guido Mastrobuoni, Dr. Elena Michelucci and Dr. Angela Casini for ESIMS spectra at University of Florence. P.Z., F.L. and F.F.B. gratefully acknowledge the financial support of the University of Siena (PAR 2008).

- [1] W. Maverick, S. C. Buckingham, Q. Yao, J. R. Bradbury, G. G. Stanley, *J. Am. Chem. Soc.* **1986**, *108*, 7430–7431.
- [2] J. Padilla, G. Gatteschi, P. Chaudhuri, *Inorg. Chim. Acta* **1997**, *260*, 217–220.
- [3] F. S. McQuillan, H. Chen, A. Hamor, C. J. Jones, *Polyhedron* **1996**, *15*, 3909–3913.
- [4] R. V. Slove, D. I. Yoon, R. M. Calhoun, J. T. Hupp, *J. Am. Chem. Soc.* **1995**, *117*, 11813–11814.
- [5] P. J. Stang, B. Olenyuk, *Acc. Chem. Res.* **1997**, *30*, 502–518; A. Kumar, S.-S. Sun, A. J. Lees, *Coord. Chem. Rev.* **2008**, *252*, 922–939; S. Tashiro, M. Tominaga, M. Kawano, B. Therrien, T. Ozeki, M. Fujita, *J. Am. Chem. Soc.* **2005**, *127*, 4546–4547; J. L. Boyer, L. M. Kuhlman, T. B. Rauchfuss, *Acc. Chem. Res.* **2007**, *40*, 233–242.
- [6] “Phosphine, Arsine and Stibine Complexes of the Transition Elements”: C. A. McAuliffe, W. Levason, *Studies in Inorganic Chemistry, Vol. 1*, Elsevier, Amsterdam, **1978**; “Catalytic Aspects of Metal Phosphine Complexes”: C. E. Alyea, D. W. Meek, *Advances in Chemistry Series, Vol. 196*, ACS, Washington, **1982**; F. A. Cotton, G. Wilkinson, C. A. Murillo, M. Bochman, *Advanced Inorganic Chemistry*, Wiley, New York **1999**; H. A. Mayer, W. C. Kaska, *Chem. Rev.* **1994**, *94*, 1239–1272.
- [7] T. De Simone, R. S. Dickson, B. W. Skelton, A. W. White, *Inorg. Chim. Acta* **1992**, *240*, 323–333; P. D. Beer, *Chem. Commun.* **1996**, 689–696; T. Baumgartner, K. Huynh, S. Schleidt, A. J. Lough, I. Manners, *Chem. Eur. J.* **2002**, *8*, 4622–4632; F.-E. Hong, Y.-J. Ho, Y.-C. Chang, Y.-C. Lai, *Tetrahedron* **2004**, *60*, 2639–2645.
- [8] E. C. Constable, C. E. Housecroft, B. Krattinger, M. Neuburger, M. Zehnder, *Organometallics* **1999**, *18*, 2565–2567.

- [9] C. J. Adams, M. I. Bruce, B. W. Skelton, A. H. White, *Inorg. Chem.* **1992**, *31*, 3336–3338; J. R. Berenguer, M. Bernechea, J. Forniés, A. García, E. Lalinde, *Organometallics* **2004**, *23*, 4288–4300; P. Álvarez, E. Lastra, J. Gimeno, P. Braña, J. A. Sordo, J. Gomez, L. R. Falvello, M. Bassetti, *Organometallics* **2004**, *23*, 2956–2966.
- [10] A. B. Chaplin, R. Scoppelitti, P. Dyson, *Eur. J. Inorg. Chem.* **2005**, 4762–4774.
- [11] H. C. Clark, G. Ferguson, P. N. Kapoor, M. Parvez, *Inorg. Chem.* **1985**, *24*, 3924–3928; W. Oberhauser, C. Bachmann, T. Stampfl, P. Brüggeler, *Inorg. Chim. Acta* **1997**, *256*, 223–224; D. Xu, H. J. Murfee, W. E. van de Veer, B. Hong, *J. Organomet. Chem.* **2000**, *596*, 53–63; L. R. Falvello, J. Forniés, J. Gómez, E. Lalinde, A. Martín, F. Martínez, M. T. Moreno, *J. Chem. Soc. Dalton Trans.* **2001**, 2132–2140.
- [12] R. V. Slove, K. D. Benkstein, S. Bélanger, J. T. Hupp, I. A. Guzei, A. L. Rheingold, *Coord. Chem. Rev.* **1998**, *171*, 221–243.
- [13] R. Nast, H. Grouhi, *J. Organomet. Chem.* **1979**, *182*, 197–202.
- [14] I. P. Beletskaya, V. V. Afanasiev, M. A. Kazankova, I. V. Efimova, *Org. Lett.* **2003**, *5*, 4309–4311.
- [15] D. Gelman, L. Jiang, S. L. Buchwald, *Org. Lett.* **2002**, *4*, 2315–2318; D. Prim, J.-M. Campagne, D. Joseph, B. Andrioletti, *Tetrahedron* **2002**, *58*, 2041–2075; D. V. Allen, D. Venkataraman, *J. Org. Chem.* **2003**, *68*, 4590–4593.
- [16] B. Liu, K. K. Wang, J. L. Petersen, *J. Org. Chem.* **1996**, *61*, 8503–8507.
- [17] M. I. Bruce, C. Hameister, A. G. Swincer, R. C. Wallis, *Inorg. Synth.* **1982**, *21*, 78–80.
- [18] J. H. Nelson, *Coord. Chem. Rev.* **1995**, *139*, 245–280.
- [19] C. G. Arena, D. Drago, M. Panzalorto, G. Bruno, F. Faraone, *Inorg. Chim. Acta* **1999**, *292*, 84–95; G. Süß-Fink, B. Therrien, *Organometallics* **2007**, *26*, 766–774; K. Pachhunga, B. Therrien, K. A. Kreisel, G. P. A. Yap, M. R. Kollipara, *Polyhedron* **2007**, *26*, 3638–3644.
- [20] M. J.-L. Tschan, F. Chérioux, B. Therrien, G. Süß-Fink, *Eur. J. Inorg. Chem.* **2007**, 509–513.
- [21] > J. P. Fackler, *Metal–Metal Bonds and Clusters in Chemistry and Catalysis*, Plenum Press, New York, **1990**; R. D. Adams, F. A. Cotton, *Catalysis by Di- and Polynuclear Metal Cluster Complexes*, Wiley-VCH, Weinheim, **1998**; M. Di Vaira, S. S. Costantini, F. Mani, M. Peruzzini, P. Stoppioni, *J. Organomet. Chem.* **2004**, *689*, 1757–1762; Y. Miyake, S. Endo, M. Yuki, Y. Tanabe, Y. Nishibayashi, *Organometallics* **2008**, *27*, 6039–6042.
- [22] The enthalpic preference for the cyclic structure over the linear one may be explained from the higher bond energy due to the increased number of M–L bonds per complex subunit. For example, the cyclic tetramer  $[(\text{CpRu}(\text{PPh}_3)(m\text{-dppab}))_4](\text{PF}_6)_4$  contains two metal–phosphorus bonds per each Ru(*m*-dppab) subunit, whereas the corresponding linear tetraruthenium chain has only 1.75 ruthenium–phosphorus bonds per Ru(*m*-dppab) subunit.
- [23] D. S. Lawrence, T. Jiang, M. Levett, *Chem. Rev.* **1995**, *95*, 2229–2260; X. Chi, A. J. Guerin, R. A. Haycock, C. A. Hunter, L. D. Sarson, *J. Chem. Soc. Chem. Commun.* **1995**, 2563–2565; X. Chi, A. J. Guerin, R. A. Haycock, C. A. Hunter, L. D. Sarson, *J. Chem. Soc. Chem. Commun.* **1995**, 2567–2569.
- [24] M. A. Galindo, M. Quirós, M. A. Romero, J. A. R. Navarro, *J. Inorg. Biochem.* **2008**, *102*, 1025–1032.
- [25] W. Y. Chan, T. Baumgartner, A. J. Lough, I. Manners, *Acta Crystallogr. Sect. E* **2007**, *63*, m2886; T. Baumgartner, K. Huynh, S. Schleidt, A. J. Lough, I. Manners, Private communication to the Cambridge Structural Database deposition number CCDC 661295.
- [26] G. Hogarth, T. Norman, *J. Chem. Soc. Dalton Trans.* **1996**, 1077–1085.
- [27] A. Grirrane, A. Pastor, A. Galindo, A. Orlandini, D. DelRio, C. Mealli, A. Ienco, A. Caneschi, J. F. Sanz, *Angew. Chem.* **2005**, *117*, 3495–3498; *Angew. Chem. Int. Ed.* **2005**, *44*, 3429–3432.
- [28] K. Wärnmark, O. Heyke, J. A. Thomas, J.-M. Lehn, *Chem. Commun.* **1996**, 2603–2604; T. J. Rutherford, O. von Gijte, A. K.-D. Mesmaeker, F. R. Keene, *Inorg. Chem.* **1997**, *36*, 4465–4474; F. R. Keene, *Chem. Soc. Rev.* **1998**, *27*, 185–193; T. J. Rutherford, F. R. Keene, *J. Chem. Soc. Dalton Trans.* **1998**, 1155–1162; H. Sato, J. Kameda, Y. Fukuda, M. Haga, A. Yamagishi, *Chem. Lett.* **2008**, *37*, 716–717; V. Chandrasekhar, R. Azhakar, S. Zucchini, J. F. Bickley, A. Steiner, *Inorg. Chem.* **2009**, *48*, 4608–4615.
- [29] D. Devanne, P. H. Dixneuf, *J. Organomet. Chem.* **1990**, *390*, 371–378; M. A. Bennett, A. J. Edwards, J. R. Harper, T. Khimyak, A. C. Willis, *J. Organomet. Chem.* **2001**, *629*, 7–18; R. Bhalla, C. J. Boxwell, S. B. Duckett, P. J. Dyson, D. G. Humphrey, J. W. Steed, P. Suman, *Organometallics* **2002**, *21*, 924–928; B. Therrien, L. Vieille-Petit, J. Jeanette-Gris, P. Stepnicka, G. Süß-Fink, *J. Organomet. Chem.* **2004**, *689*, 2456–2463.
- [30] P. Zanello, *Inorganic Electrochemistry. Theory, Practice and Application*, RSC, Cambridge, **2003**.
- [31] S. Santi, L. Broccardo, M. Bassetti, P. Alvarez, *Organometallics* **2003**, *22*, 3478–3484.
- [32] “Electron Paramagnetic Resonance of d Transition Metal Compounds”: F. E. Mabbs, D. Collison, *Studies in Inorganic Chemistry, Vol. 16*, Elsevier, New York, **1992**; J. R. Pilbrow, *Transition Ion Electron Paramagnetic Resonance*, Oxford Science Publication, Oxford, **1990**; R. S. Drago, *Physical Methods for Chemists*, Saunders College, New York, **1992**.
- [33] D. Osella, G. Arman, R. Gobetto, F. Laschi, P. Zanello, S. A. S. V. Goodfellow, C. E. Housecroft, S. M. Owen, *Organometallics* **1989**, *8*, 2689–2695; C. Bianchini, M. Peruzzini, A. Ceccanti, L. Laschi, P. Zanello, *Inorg. Chim. Acta* **1997**, *259*, 61–70; P. Diversi, M. Fontani, M. Fuligni, F. Laschi, S. Matteoni, C. Pinzino, P. Zanello, *J. Organomet. Chem.* **2001**, *626*, 145–156.
- [34] CU23GPN1 Simulation Program, M. Romanelli.
- [35] S. Takahashi, Y. Kuroyama, K. Sonogashira, N. Hagihara, *Synthesis* **1980**, 627–630.
- [36] S. Leininger, J. Stang, *Organometallics* **1998**, *17*, 3981–3987.
- [37] A. G. Alonso, L. B. Reventós, *J. Organomet. Chem.* **1988**, *338*, 249–254.
- [38] M. Krejčík, M. Daněk, F. Hartl, *J. Electroanal. Chem.* **1991**, *317*, 179–187.
- [39] O.D.L. CrysAlisCCD, Version 1.171.31.2, CrysAlis171.NET, **2006**.
- [40] O.D.L. CrysAlis RED, Version 1.171.31.2, CrysAlis171.NET, **2006**.
- [41] A. Altomare, M. C. Burla, M. Cavalli, G. L. Cascarano, C. Giacovazzo, A. Guagliardi, A. G. G. Moliterni, G. Polidori, R. Spagna, *J. Appl. Crystallogr.* **1999**, *32*, 115–119.
- [42] G. M. Sheldrick, *Acta Crystallogr. Sect. A* **2008**, *64*, 112–122.
- [43] M. Nardelli, *Comput. Chem.* **1983**, *7*, 95–98.
- [44] M.N.B.a.C.K.J. ORTEP-III, Report ORNL-6895, Oak Ridge National Laboratory, Oak Ridge, **1996**; L. J. Farrugia, *J. Appl. Chem.* **1997**, *47*, 565.
- [45] L. J. Farrugia, *J. Appl. Chem.* **1999**, *49*, 837–838.

Received: June 16, 2009  
Published online: September 29, 2009